

Surface Organometallic Chemistry of Titanium: Synthesis, Characterization, and Reactivity of $(\equiv\text{Si}-\text{O})_n\text{Ti}(\text{CH}_2\text{C}(\text{CH}_3)_3)_{4-n}$ ($n = 1, 2$) Grafted on Aerosil Silica and MCM-41

Fabien Bini,[†] Cécile Rosier,^{†,§} Romain Petroff Saint-Arroman,^{†,||} Eva Neumann,^{†,⊥} Céline Dablemont,[†] Aimery de Mallmann,^{*,†} Frédéric Lefebvre,[†] Gerald P. Niccolai,^{†,‡} Jean-Marie Basset,^{*,†} Mark Crocker,^{‡,△} and Jan-Karel Buijink[‡]

Laboratoire de Chimie Organométallique de Surface (UMR 9986 CNRS/ENSCE Lyon) 43, boulevard du 11 novembre 1918, 69616 Villeurbanne Cedex, France, and Shell International Chemicals, Shell Research and Technology Center Amsterdam, P.O. Box 38000, 1030 BN Amsterdam, The Netherlands

Received August 4, 2005

The reaction of tetrakisneopentyl titanium, TiNp_4 (**1**), with the surface of partially dehydroxylated Aerosil silica and MCM-41 and the reactivity of the resultant supported titanium alkyl product with water, alcohols, and oxygen are reported. Two methods of preparation have been investigated and compared for the grafting of TiNp_4 : (i) reaction of the support with the vapor of the sublimed complex and (ii) impregnation of the support with a solution of the complex. The second method appeared to be more reliable for “larger scale” preparations. The surface species thus obtained were characterized by infrared spectroscopy, solid state NMR, XAFS, elemental analysis, and various test reactions. Whereas on an Aerosil silica partially dehydroxylated at 500 °C, $\text{SiO}_{2-(500)}$, the surface complex is a monopodal titanium trisalkyl complex, $\equiv\text{SiO}-\text{Ti}[\text{CH}_2\text{C}(\text{CH}_3)_3]_3$, **2a**, a bipodal titanium bisalkyl complex, $(\equiv\text{SiO})_2\text{Ti}[\text{CH}_2\text{C}(\text{CH}_3)_3]_2$, **2b**, is obtained as the major species (ca. 65%) with **2a** on MCM-41₍₅₀₀₎. The reason for this difference in behavior is discussed on the basis of the surface structure. The results obtained from hydrolysis confirmed the structure proposed for the supported alkyl complexes. For the reaction of the alkyl surface complexes with alcohols (MeOH, EtOH, *t*BuOH), the surface compounds obtained were characterized by the same techniques and by XPS and UV–vis. The results are consistent with the formation of monosiloxytrisalkoxy titanium complexes on $\text{SiO}_{2-(500)}$, $\equiv\text{SiO}-\text{Ti}(\text{OR})_3$, **3a_{OR}**, and of $\equiv\text{SiO}-\text{Ti}(\text{O}^i\text{Bu})_3$, **3a_{OⁱBu}**, and $(\equiv\text{SiO})_2\text{Ti}(\text{O}^i\text{Bu})_2$, **3b_{OⁱBu}**, on MCM-41₍₅₀₀₎, after reaction with *t*BuOH. The supported titanium alkyl, **2a**, also reacts with oxygen, leading mainly to $\equiv\text{SiO}-\text{Ti}[\text{OCH}_2\text{C}(\text{CH}_3)_3]_3$, probably via an unstable surface compound such as $\equiv\text{SiO}-\text{Ti}[\text{OCH}_2\text{C}(\text{CH}_3)_3]_2[\text{OOCH}_2\text{C}(\text{CH}_3)_3]$, resulting from the incorporation of two molecules of oxygen in **2a**.

Introduction

Surface organometallic chemistry (SOMC) is an area of heterogeneous catalysis that has emerged as a result of a comparative analysis of homogeneous and heterogeneous catalysis.¹ The chemical industry has often favored heterogeneous catalysis, but the development of better catalysts is frequently hindered by the presence of numerous kinds of active sites and also by their low concentration. By reacting organometallic compounds with oxide surfaces, one tries to generate “single-

site” species, that is, sites that have the same chemical environment, to elaborate new catalysts.^{2–8}

Concerning group IV elements, silica-supported zirconium^{9–11} alkyl and hydride complexes have been synthesized and well

* To whom correspondence should be addressed. E-mail: basset@cpe.fr; demallmann@cpe.fr. Phone: +33(0)47243 1794/1802 /1807. Fax: +33-(0)47243 1795.

[†] Laboratoire de Chimie Organométallique de Surface.

[‡] Shell International Chemicals.

[§] Present address: Rhodia, CRTL, BP 62, 69192 Saint-Fons, France.

^{||} Present address: Rhodia Polyamide, avenue Ramboz, 69192 Saint-Fons, France.

[⊥] Present address: University of Basel, Department of Chemistry, Organic Chemistry, St. Johanns-Ring 19, CH-4056 Basel, Switzerland.

[‡] Present address: UMR ICAR, Université Lumière Lyon 2–ENS LSH–ENS Lyon–INRP, 15, parvis René Descartes, 69342 Lyon Cedex 7, France.

[△] Present address: Center for Applied Energy Research, University of Kentucky, 2540 Research Park Dr., Lexington, KY 40511-8410.

(1) Copéret, C.; Chabanas, M.; Petroff Saint-Arroman, R.; Basset, J. M. *Angew. Chem., Int. Ed.* **2003**, *42*, 156–181.

(2) Dufaud, V.; Basset, J. M. *Angew. Chem., Int. Ed.* **1998**, *37*, 806–810.

(3) Vidal, V.; Theolier, A.; Thivolle-Cazat, J.; Basset, J. M. *Science* **1997**, *276*, 99–102.

(4) Soulivong, D.; Copéret, C.; Thivolle-Cazat, J.; Basset, J. M.; Maunders, B. M.; Parly, R. B. A.; Sunley, G. J. *Angew. Chem., Int. Ed.* **2004**, *43*, 5366–5369.

(5) Basset, J. M.; Bres, P.; Copéret, C.; Maunders, B.; Soulivong, D.; Taoufik, M.; Thivolle-Cazat, J. French Patent FR 2840607, 2003.

(6) Chabanas, M.; Baudouin, A.; Copéret, C.; Basset, J. M. *J. Am. Chem. Soc.* **2001**, *123*, 2062–2063.

(7) (a) Capdevielle, V. Ph.D. Thesis, University Claude Bernard-Lyon I, Villeurbanne, France, 1996. (b) Ferret, N.; Dufaud, V.; Salinier, V.; Basset, J. M. French Patent FR 2747675, 1997.

(8) Meunier, D.; Piechaczyk, A.; de Mallmann, A.; Basset, J. M. *Angew. Chem., Int. Ed.* **1999**, *38*, 3540–3542. Yang, Q.; Coperet, C.; Li, C.; Basset, J. M. *New J. Chem.* **2003**, *27*, 319–323.

(9) Quignard, F.; Lecuyer, C.; Bougault, C.; Lefebvre, F.; Choplin, A.; Olivier, D.; Basset, J.-M. *Inorg. Chem.* **1992**, *31*, 928–930.

(10) Lecuyer, C. Ph.D. Thesis, University Claude Bernard-Lyon I, Villeurbanne, France, 1992.

(11) Corker, J.; Lefebvre, F.; Lecuyer, C.; Dufaud, V.; Quignard, F.; Choplin, A.; Evans, J.; Basset, J.-M. *Science* **1996**, *271*, 966–969.

characterized, while only preliminary results were obtained in the case of similar supported titanium¹² and hafnium¹³ complexes. For example, the reaction of tetrakisneopentyl zirconium, $Zr(CH_2C(CH_3)_3)_4$, with a silica surface partially dehydroxylated at 500 °C, $SiO_{2-(500)}$, leads to the formation of only one type of monopodal (or monosiloxy: one bond with the silica surface) surface species, $\equiv SiO-Zr(CH_2C(CH_3)_3)_3$. This surface complex was characterized by infrared and MAS 1H and ^{13}C NMR spectroscopies, EXAFS, elemental analysis, and a wide variety of chemical assays. The same reactivity was observed in the reaction between tetrakisneopentyl hafnium and $SiO_{2-(500)}$,^{13,14} and the grafted complex obtained has been characterized by a number of different techniques. In the case of hafnium, the grafting reaction was also carried out using a silica dehydroxylated at 250 °C, $SiO_{2-(250)}$, and it was found that the reaction leads to a bipodal bisalkyl complex, $(\equiv SiO)_2Hf(CH_2C(CH_3)_3)_2$. Another way to form multipodal surface metal complexes is through the reaction of these surface alkyl complexes with hydrogen at 150 °C, a phenomenon that we have been studying for a long time.^{1,9-11,15,16} Starting from monopodal zirconium trisalkyl species, $\equiv SiO-Zr(CH_2C(CH_3)_3)_3$, tripodal (major) and bipodal (minor) silica-supported hydride species, $(\equiv SiO)_{4-x}ZrH_x$ ($x = 1, 2$), were thus obtained.¹⁷ It has then been established that monopodal (alkyls) and multipodal (alkyls, hydrides) zirconium or hafnium complexes in their +4 oxidation state can be selectively formed on the silica surface. Furthermore, these alkyls and hydrides can be converted into a variety of alkoxides by the simple reaction of the surface complex with alcohols. The interest of the extension of this chemistry to titanium, for application to olefin epoxidation, is obvious, and the development of the basic surface organometallic chemistry of titanium on Aerosil and MCM-41 has been pursued in our group. In the case of titanium, silica-supported complexes have already been prepared by methods very similar to our own: Catalysts were derived from $\equiv SiO-Ti(CH_2C(CH_3)_3)_3$ ¹⁸ and mono- or dimeric titanium amido or alkoxy surface complexes¹⁹ such as $\equiv SiO-Ti(NEt_2)_3$, $(\equiv SiO)_2Ti(NEt_2)_2$, $\equiv SiO-Ti(O^iPr)_3$, $(\equiv SiO)_2Ti(O^iPr)_2$, $[\equiv SiO-Ti(O^iPr)_2]_2O$, and $\equiv SiO-Ti(O^iPr)_2(\mu-O)Ti(O^iPr)_3$.

Oxide-supported titanium complexes and titanium silicalites are of considerable interest due to their activity for the oxidation of various substrates.²⁰⁻²² In the epoxidation of propene by the Shell SMPO process, propene reacts with an alkyl hydroperoxide over a catalyst based on titanium(IV) sites supported on silica.²³

It is now generally accepted that the active site of this type of catalysts involves isolated open lattice sites, that is, tetrahedral isolated titanium(IV) centers linked to the surface by three siloxy bridges.²⁴ The synthetic titanium silicalite, TS-1, catalyzes the epoxidation by hydrogen peroxide of several olefins, and again the reactive sites invoked are mononuclear titanium(IV) centers.²⁵ However, large organic molecules cannot have access to the active sites located inside the micropores of the zeolites. The discovery of ordered mesoporous silicates such as MCM-41²⁶ allowed the use of alkyl peroxides as oxidants and to catalyze the epoxidation of a wider range of substrates by titanium-substituted molecular sieves materials.²⁷ Mesoporous TiO_2-SiO_2 mixed oxide aerogels²⁸ are also good epoxidation catalysts when associated with alkyl hydroperoxide as oxidants.^{29,30} However, in these synthetic mesoporous solids, not all the titanium atoms are accessible to the substrates since they can be embedded into the walls of the structure and the introduction of titanium onto the surface of the mesoporous oxides by postsynthesis methods generally provides larger amounts of active sites. For instance molecular precursor approaches involving the deposit of titanocene dichloride in the interior of a MCM-41 mesoporous silica³¹ or the grafting of siloxy titanium complexes such as $(^iPrO)Ti[OSi(O^iBu)_3]_3$ within MCM-41 and SBA-15³² were developed and produced site-isolated titanium epoxidation catalysts of high activity and selectivity. In parallel, interesting studies have appeared using soluble models of the silica surface, partially condensed polyoligosilsesquioxanes, to perform detailed in situ catalytic studies of the epoxidation of olefins by alkyl hydroperoxides catalyzed by titanium(IV) siloxides.³³⁻³⁵

In the present publication we report the comparative study of the first step of the synthesis of titanium catalysts by surface organometallic chemistry: The grafting of tetrakisneopentyl titanium, $Ti(Np)_4$, on (i) a nonporous amorphous Aerosil silica and (ii) a mesoporous MCM-41 silica partially dehydroxylated at different temperatures. Two ways of preparation, referred to as sublimation and impregnation methods, have been investigated. The reaction of the organometallic precursor with the oxide surface will be analyzed, the silica-supported titanium species will be characterized, and their evolution with temperature will be studied. The primary objective of this work was the production of well-characterized, monopodal $\equiv SiO-TiNp_3$ - or eventually bipodal $(\equiv SiO)_2TiNp_2$ -supported precursors. These grafted titanium neopentyl species will then be reacted with

(12) Rosier, C.; Niccolai, G.; Basset, J. M. *J. Am. Chem. Soc.* **1997**, *119*, 12408–12409.

(13) d'Ornelas, L.; Reyes, S.; Quignard, F.; Choplin, A.; Basset, J.-M. *Chem. Lett.* **1993**, 1931–1934.

(14) Reyes, S. Ph.D. Thesis, Universidad Central de Venezuela, Caracas, 1997.

(15) (a) Quignard, F.; Choplin, A.; Basset, J. M. *J. Chem. Soc., Chem. Commun.* **1991**, 22, 1589–1590. (b) Lecuyer, C.; Quignard, F.; Choplin, A.; Olivier, D.; Basset, J. M. *Angew. Chem., Int. Ed. Engl.* **1991**, *30*, 1660–1661.

(16) These resulting silica-supported zirconium and hafnium(IV) hydride species are active for the hydrogenolysis of carbon–carbon bonds under very mild conditions of temperature and pressure.

(17) (a) Thieuleux, C.; Quadrelli, E. A.; Basset, J. M.; Doebler, J.; Sauer, J. *Chem. Commun.* **2004**, 1729–1731. (b) Rataboul, F.; Baudouin, A.; Thieuleux, C.; Veyre, L.; Copéret, C.; Thivolle-Cazat, J.; Basset, J. M.; Lesage, A.; Emsley, L. *J. Am. Chem. Soc.* **2004**, *126*, 12541–12550.

(18) Holmes, S. A.; Quignard, F.; Choplin, A.; Teissier, R.; Kervennal, J. *J. Catal.* **1998**, *176*, 173–181 and 182–191.

(19) Bouh, A.; Rice, G. L.; Scott, S. L. *J. Am. Chem. Soc.* **1999**, *121*, 7201–7210.

(20) Notari, B. *Catal. Today* **1993**, *18*, 163–172.

(21) Arends, I. W. C. E.; Sheldon, R. A. *Appl. Catal. A* **2001**, *212*, 175–187.

(22) Brégeault, J. M. *J. Chem. Soc., Dalton Trans.* **2003**, 3289–3302.

(23) Wulff, H. P. (Shell Oil) UK Patent 1,249,079, 1971.

(24) Buijink, J. K. F.; van Vlaanderen, J. J. M.; Crocker, M.; Niele, F. G. M. *Catal. Today* **2004**, *93–95*, 199–204.

(25) Bellussi, G.; Rigutto, M. S. *Stud. Surf. Sci. Catal.* **1994**, *85*, 177–213.

(26) Beck, J. S.; Vartuli, J. C.; Roth, W. J.; Leonowicz, M. E.; Kresge, C. T. *J. Am. Chem. Soc.* **1992**, *114*, 10834–10843. Kresge, C. T.; Leonowicz, M. E.; Roth, W. J.; Vartuli, J. C.; Beck, J. S. *Nature* **1992**, *359*, 710–712.

(27) Corma, A.; Navaro, M. T.; Pérez-Pariente, J. Spanish patent 9301327, 1993. Corma, A.; Navaro, M. T.; Pérez-Pariente, J. *J. Chem. Commun.* **1994**, 147–148.

(28) Dutoit, D. C. M.; Schneider, M.; Baiker, A. *J. Catal.* **1995**, *153*, 165–176.

(29) Dutoit, D. C. M.; Schneider, M.; Hutter, R.; Baiker, A. *J. Catal.* **1996**, *161*, 651–658.

(30) Kochkar, H.; Figueras, F. *J. Catal.* **1997**, *171*, 420–430.

(31) Maschmeyer, T.; Rey, F.; Sankar, G.; Thomas, J. M. *Nature* **1995**, *378*, 159–162.

(32) Jarupatrakorn, J.; Tilley, T. D. *J. Am. Chem. Soc.* **2002**, *124*, 8380–8388.

(33) Abbenhuis, H. C. L.; Krijnen, S.; van Santen, R. *Chem. Commun.* **1997**, 331–332.

(34) Crocker, M.; Herold, R. H. M.; Orpen, A. G.; Overgaag, M. T. A. *Chem. Commun.* **1997**, 2411–2412.

(35) Crocker, M.; Herold, R. H. M.; Orpen, A. G.; Overgaag, M. T. A. *J. Chem. Soc., Dalton Trans.* **1999**, 3791–3804.

Table 1. Quantification of the Gases Evolved during the Grafting of TiNp₄ onto Different Supports

support	OH density, OH/nm ² ^a (surface area, m ² /g) ^b	wt % Ti	% SiOH consumed	[NpH (+ NpD)]/Ti	NpD/Ti	NpD/ (NpH + NpD)	n ^c
Preparation by Sublimation							
SiO ₂ -(500) IR disk	1.3 (200)	1.4–1.8	70–100%	3.47	1.04 ^d	30%	1.04 ^d
SiO ₂ -(500) powder	1.3 (200)	0.4–0.8	20–50%	1.35	1.12 ^d	83%	1.12 ^d
Preparation by Impregnation (powders)							
SiO ₂ -(200)	2.35 (200)	1.2–1.6	45–70%	1.4–1.6			1.55 ^e
SiO ₂ -(500)	1.3 (200)	1.2–1.6	60–95%	1.05–1.10	1.07 ^e	100%	1.07 ^e
SiO ₂ -(700)	0.7 (190)	1.1–1.2	95–100%	1.00			1.00 ^e
MCM41(200)	2.5 (1060)	3.6–4.0	35–50%	2.05			2.05 ^e
MCM41(500)	1.2 (1060)	3.4–4.0	60–85%	1.55–1.80			1.65 ^e

^a ±10%. ^b ±5 m²/g for Aerosil silica and ±30 m²/g for MCM-41. ^c n, in the formula (≡SiO)_nTi(Np)_{4-n}, is an average value determined from the results obtained by gas evolution during the grafting reaction, NpH/Ti for preparations by the impregnation method or NpD/Ti for preparations by the sublimation method. ^d ±20%. ^e ±12%.

several oxygenated molecules such as dioxygen, water, and alcohols to synthesize hydroxy and alkoxy and possibly peroxy titanium-supported catalysts since our ultimate goal is the production of catalysts for the epoxidation of olefins or the decomposition of hydroperoxides. The conversion of the mono- or bipodal complexes to tripodal complexes, better anchored onto the silica surface and thus less sensitive to leaching, is treated in a second paper in this series. The catalytic activity of the different supported titanium complexes will be studied in other reports.

Experimental Section

1. General Procedures. All manipulations and reactions were conducted under a strict inert atmosphere or vacuum. Sealed tube reactors and break-seal techniques were used throughout. Infrared spectra were recorded on a Nicolet FT-IR Magna 550 spectrometer equipped with a cell designed for in situ preparations under controlled atmosphere. Solid state NMR studies were carried out on 300 and 500 MHz Bruker spectrometers. For all experiments, the rotation frequency was set to 10 kHz. Chemical shifts are given with respect to TMS as an external standard, with a precision of 0.2–0.3 and 1 ppm for ¹H and ¹³C NMR, respectively. Parameters used for (i) ¹H MAS NMR spectra: pulse delay, 2 s; 8 to 32 scans per spectrum; (ii) ¹³C CP/MAS NMR spectra: 90° pulse on the protons (impulsion length 3.8 μs), then a cross-polarization step with a contact time typically set to 5 ms and finally recording of the ¹³C signal under high-power proton decoupling; pulse delay, 2 s; 20 000 to 100 000 scans per spectrum; an apodization function (exponential) corresponding to a line-broadening of 50 Hz was applied to the spectrum. Air-sensitive samples were transferred within a glovebox into a tightly closed zirconia rotor. ESR X-band spectra were recorded at a temperature of 77 K on a JEOL (RE2X) spectrometer with a frequency of ca. 9.5 GHz. For a quantitative evaluation, the integration of the absorbance spectrum was performed and compared to the integration of the spectrum of a vanadyl sulfate standard. X-ray photoelectron (XPS) spectra were recorded on a Kratos XSAM 800 spectrometer employing the C 1s line (285.0 eV) as a binding energy standard. The UV–vis spectrum was recorded in air (with a total exposure time of ca. 10 min for the sample) on a Perkin-Elmer 320 spectrometer operating in the diffuse reflectance spectral mode. Elemental analyses were performed at the Catalysis Research Institute (IRC, Villeurbanne, France), the Central Analysis Service of the CNRS (Solaize, France), or Pascher Laboratory (Remagen, Germany) in the case of extremely sensitive products.

Two oxide supports were used: Aerosil 200 silica from Degussa and a MCM-41. Aerosil 200 is a nonporous flame silica, in the form of regular particles of an average diameter of 150 Å and free of halide impurities. It was dehydroxylated under vacuum (10⁻⁵ mbar) at 500 or 700 °C for a minimum of 15 h, leading to SiO₂-(500) or SiO₂-(700) support, respectively. A SiO₂-(200) sample was prepared

by rehydration of SiO₂-(500) at room temperature and heating statically at 100 °C for 4 h followed by a dehydroxylation at 200 °C for 15 h. The mesoporous MCM-41 support was prepared according to a classical procedure³⁶ and presented a narrow pore size distribution (2.5–4.0 nm) centered around 3.2 nm. It was first calcined at 500 °C and then treated under vacuum at the same temperature for 15 h, leading to MCM-41(500). A MCM-41(200) sample was prepared from MCM-41(500) with the same method described above for the preparation of the SiO₂-(200) support. The specific surface areas of the Aerosil silica and MCM-41 supports are reported in Table 1, with the corresponding densities of hydroxyl groups per nm², determined by quantitative solid state ¹H MAS NMR³⁷ and chemical titration with CH₃Li, CH₃MgBr, or LiAlH₄. When an experiment required deuterated silica, the following procedure was applied: SiO₂-(500) was reacted with D₂O (*P* = 22 Torr) at 500 °C for 1 h, followed by evaporation under vacuum at the same temperature for 1 h. This procedure was repeated twice before a final dehydroxylation of the silica under vacuum at 500 or 700 °C for 15 h. According to quantitative IR data (comparison between the intensity of the band at 3747 cm⁻¹, ν(SiO–H), before and after the treatment with D₂O), the silica was more than 95% deuterated.

Other starting materials were obtained from Aldrich (lithium, titanium tetrachloride, methanol, and *tert*-butyl alcohol) or Lancaster (neopentyl chloride). Neopentyl chloride, oxygen gas, methanol, and *tert*-butyl alcohol were dried and stored over molecular sieves. Tetrakisneopentyl titanium (**1**) was synthesized as described by Mowat and Wilkinson³⁸ in about 25% yield.

2. Reaction of TiNp₄ with SiO₂ and MCM-41. Two types of preparation were investigated. For IR experiments (ca. 15 mg pellets) the reaction was mainly carried out by the direct sublimation of the organometallic precursor on the support (in the following, this method is called “sublimation”). For larger amounts of supports (ca. 0.2 to 1 g), the reaction was carried out by impregnating the support powder with a pentane solution of TiNp₄ (in the following, this method is called “impregnation”). In the case of large amounts

(36) The MCM-41 support was provided by Shell Chemicals Research and Technology Centre of Amsterdam. Below is a short summary of its preparation method: 457 g of cetyltrimethylammonium bromide was mixed with 2857 g of water and 784 g of a 25% water solution of tetramethylammonium hydroxide. After addition of 1300 g of tetramethyl orthosilicate, the mixture was stirred for 3 h at room temperature. The precipitate was filtered off and washed with distilled water until the water presented a neutral pH. To remove most of the template by acid/solvent extraction, the precipitate was then suspended and washed in 5 L of a 0.1 M solution of HCl in ethanol, warmed to 60 °C while stirring, kept at 60 °C for 1 h, cooled to 40 °C, stirred during an additional 5 h, and finally filtered. This ion-exchange procedure was repeated, and the solid was dried at 120 °C for 4 h, then heated to 540 °C (50 °C/h), and calcined at this temperature for 2 h.

(37) Millot, N.; Santini, C. S.; Lefebvre, F.; Basset, J. M. *C. R. Chim.* **2004**, *7*, 725–736.

(38) Mowat, W.; Wilkinson, G. *J. Chem. Soc., Dalton Trans.* **1973**, 1120–1124.

of SiO₂-(500), both methods were used in order to study their reproducibility and the effect of the solvent.

2.a. Process for a Reaction by Sublimation in an Infrared Cell. TiNp₄ (5–10 mg) was introduced under argon into a tube reactor with a break-seal. This tube was sealed under vacuum and then sealed perpendicularly to the infrared cell consisting of a long, closed ϕ 30 mm glass tube with CaF₂ windows and a stopcock at one end. The infrared cell contained a mobile cylindrical Pyrex or quartz support containing the silica disk (ca. 15 mg of silica). This support could be moved to the bottom of the cell for thermal treatments (dehydroxylation, desorption), over the break-seal tube for the sublimation of TiNp₄, and finally to the upper part of the cell, between the CaF₂ windows, for infrared spectra.

The silica disk was dehydroxylated (200, 500, or 700 °C) under vacuum (10⁻⁵ Torr), the break-seal was then opened, and the tetrakisneopentyl titanium was gently heated with a blow-dryer (50–60 °C). Condensation on the silica disk was confirmed by a color change. At the end of the sublimation, the unreacted complex was trapped at 77 K in the break-seal, which was then removed by flame sealing.

2.b. Process for a Reaction by Sublimation in a Reactor (“Large Quantities”). A break-seal tube containing TiNp₄ sealed under vacuum was sealed to a straight, closed glass tube containing silica (0.5 g) and equipped with a stopcock and a second, empty break-seal tube (for product storage). Silica was then partially dehydroxylated at 500 °C. The break-seal was then opened, and TiNp₄ was sublimed onto the silica, which was cooled in liquid nitrogen. The silica thus treated with TiNp₄ was allowed to warm to room temperature and then heated very progressively to 50–60 °C for 1 h. The gases evolved and the unreacted TiNp₄ were trapped at 77 K in the break-seal, which was then removed by sealing. The resultant supported complex was either stored in the second empty break-seal tube or used directly in the reactor for another step of a catalyst synthesis (e.g., reaction with an alcohol).

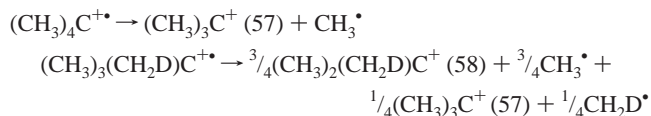
2.c. Process for a Reaction by Impregnation in a Reactor. The impregnation technique consists typically of stirring at 25 °C for 2 to 4 h a mixture of the desired support (ca. 0.5 g) and of a solution of the molecular complex in pentane (in excess compared to the number of hydroxyl groups of the support). After filtration the solid was washed three times with small aliquots of pentane and finally dried under vacuum (10⁻⁵ mmHg), at room temperature, for 15 h.

2.d. Process for a Reaction by Impregnation for Infrared Studies. After a partial dehydroxylation of the disk of support at the desired temperature (200, 500, or 700 °C) under vacuum, the infrared cell was opened in the glovebox and the SiO₂ or MCM-41 disk introduced in a pentane solution containing the organometallic complex. After ca. 1 h it was transferred in a container containing only pentane, where it was kept for 1 h for washing, thus eliminating the unreacted physisorbed TiNp₄. This washing operation was repeated three times with a new pentane solution each time. This method gave the same results as the sublimation method for IR studies but appeared to be less convenient.

3. Determination of Evolved Gases. Depending on the preparation method (sublimation or impregnation), the determination of the evolved gases (type and amount) was not carried out exactly with the same method. In the first case (sublimation), the gases were condensed at 77 K in a Schlenk tube equipped with a septum. After warming to room temperature for several hours, a sample of the gas phase was taken and analyses were performed by gas chromatography (Hewlett-Packard 5890 series II GC equipped with a flame ionization detector and a KCl/AlO₃ on fused silica column).

When necessary, mass spectroscopy was used to confirm the identification of the products. The mass spectra were recorded on a GC/MS Hewlett-Packard G1800A GCD system. Mass spectroscopy was also used to determine the ratio NpD/NpH, which is calculated from the intensity of peaks 57 and 58 (*I*₅₇ and *I*₅₈),

corresponding to the major peaks of the spectrum of neopentane, the *tert*-butyl fragment:



The molar fractions of nondeuterated neopentane (*x*_{NpH}) and deuterated neopentane (*x*_{NpD}) were calculated by fitting the data to the following relation (using the iterative “solveur” function of Microsoft Excel), based on a model allowing deuterations at only one of the neopentyl groups.

$$I_{57}/[I_{57} + I_{58}] = x_{\text{NpH}} + \frac{1}{4}x_{\text{NpD}}$$

$$I_{58}/[I_{57} + I_{58}] = \frac{3}{4}x_{\text{NpD}}$$

Analyses that allowed indiscriminate scrambling or allowed triply or quadruply deuterated methyl groups showed significantly degraded or unimproved fitting, respectively.

When the preparation was made by impregnation, it was necessary to perform the analysis differently, due to the solubility of the evolved gases (neopentane) in the solvent (pentane). For this purpose both the evolved gases and the solvent were trapped in a Schlenk tube. After warming to room temperature the Schlenk tube was connected to a large flask, allowing all the solvent to be evaporated. The analyses were then performed as above. By this way all evolved gases, even those dissolved in the solvent, could be analyzed with a good reproducibility.

4. Reactions with Water, Alcohol, and Oxygen. Liquid reagents (alcohol or water) were degassed and stored under vacuum in Schlenk tubes. Oxygen was contained in a sealed tube over activated molecular sieves. The reagent tube and the reactor (either an infrared cell or sealed tube reactor containing the grafted titanium complex) were fixed to a T-tube, which was attached to the vacuum line. The T-connection was subsequently evacuated and isolated from the vacuum line. The reactor was cooled to 77 K, and the Schlenk containing the alcohol or water was briefly opened. The reactor was then isolated and allowed to warm to room temperature. The gases evolved during the reaction were analyzed and quantified by gas chromatography. After gas sampling, the reactor was heated at 70–80 °C under dynamic vacuum (10⁻⁴ mbar) in the presence of a cold trap at 77 K (liquid nitrogen) in line, to remove the unreacted reagent.

In the case of oxygen, for volumetry experiments, the reactor and the Schlenk tube containing oxygen were connected to a vacuum line incorporating a precision pressure gauge (Texas Instruments, model 145-01) and several known volumes. A pressure of oxygen (ca. 400 Torr) was established in a known volume including the gauge. The oxygen tube was closed and the oxygen-containing volume was opened to the reactor. The evolution of the pressure was followed over 20 h, and the ideal gas law relation was used to determine the number of moles of oxygen consumed. After reaction, the volume of the reactor was determined using an inert gas, the reactor was opened, and the solid therein was weighed and submitted for titanium and carbon analysis.

5. XAFS Studies (EXAFS and XANES). The samples were packaged as pellets within an argon-filled drybox in double airtight sample holders equipped with Kapton windows. X-ray absorption spectra were acquired at the Laboratoire pour l'Utilisation du Rayonnement Electromagnétique (LURE), on the DCI ring at beam line D44, at room temperature at the titanium K edge, in the transmission mode. For XANES, the spectra were recorded from 4900 to 5200 eV using a double-crystal Si-(311) monochromator, detuned to eliminate most of the higher harmonics content of the beam, and 0.5 mm slits. The energy/angle calibration was performed using a Ti metal foil and was checked between each spectrum. The

reference for energies was chosen at 4966.4 eV for the Ti K-edge of the metal foil³⁹ (first inflection point in the Ti metal K-edge spectrum⁴⁰). With a similar calibration, Farges et al. found the position of the pre-edge peak of Ba₂TiO₄ at 4969.5 eV.⁴¹ A 0.3 eV sampling step was chosen between 4950 and 5100 eV and a 1.0 eV step before and after this energy range, with an integration time of 2.0 s per point. The experimental XANES spectra were normalized with the Athena program,⁴² by adjusting a measured spectrum to match the energy dependence of the Cromer–Lieberman calculations for the absorption of a free atom. The position of the pre-edge peak and its height were extracted from these normalized spectra. For EXAFS, a double-crystal Si–(111) monochromator was used and the spectra were recorded between 4850 and 5850 eV with a 2.0 eV step. The spectra analyzed were the result of the averaging of four such acquisitions. It was carefully checked that the results obtained by recording the spectra for XANES and EXAFS purpose were comparable and reliable since for each sample no evolution could be detected by comparing the spectra between the first and last acquisition and by comparing the absorption spectra recorded for XANES and EXAFS, which superimposed very well (except for the height of the pre-edge feature, due to lower resolution used for EXAFS⁴¹). The data analyses for EXAFS were performed by standard procedures using the programs developed by Alain Michalowicz, in particular the EXAFS fitting program RoundMidnight.⁴³ In each spectrum the postedge background subtraction was carefully conducted using polynomial or cubic-spline fittings, and the removal of the low-frequency contributions was checked by further Fourier transformation. Fitting of the spectrum was done on the k^3 - and k^1 -weighted data (a k^3 weighting is recommended when only light back-scatterers with $Z < 36$ are present⁴⁴), using the following EXAFS equation where S_0^2 is a scale factor; N_i is the coordination number of shell i ; r_c is the total central atom loss factor; F_i is the EXAFS scattering function for atom i ; R_i is the distance to atom i from the absorbing atom; λ is the photoelectron mean free path; σ_i is the Debye–Waller factor; Φ_i is the EXAFS phase function for atom i ; and Φ_c is the EXAFS phase function for the absorbing atom:

$$\chi(k) \cong S_0^2 r_c(k) \sum_{i=1}^n \frac{N_i F_i(k, R_i)}{k R_i^2} \exp\left(\frac{-2R_i}{\lambda(k)}\right) \exp(-2\sigma_i^2 k^2) \sin[2kR_i + \Phi_i(k, R_i) + \Phi_c(k)]$$

The program FEFF⁷⁴⁵ was used to calculate theoretical values for r_c , F_i , λ , and $\Phi_i + \Phi_c$ based on model clusters of atoms. The refinements were performed by fitting the structural parameters N_i , R_i , and σ_i and the energy shift, ΔE_0 (the same for all shells). The fit residue, ρ (%), was calculated by the following formula:

$$\rho = \frac{\sum_k [k^3 \chi_{\text{exp}}(k) - k^3 \chi_{\text{calc}}(k)]^2}{\sum_k [k^3 \chi_{\text{exp}}(k)]^2} \times 100$$

As recommended by the Standards and Criteria Committee of the International XAFS Society,⁴⁶ an improvement of the fit took

(39) Bearden, J. A.; Burr, A. F. *Rev. Mod. Phys.* **1967**, *39*, 125–142.

(40) Gregor, R. B.; Lytle, F. W.; Sandstrom, D. R.; Wong, J.; Schultz, P. *J. Non-Cryst. Solid* **1983**, *55*, 27–43.

(41) Farges, F.; Brown, G. E., Jr.; Rehr, J. J. *Geochim. Cosmochim. Acta* **1996**, *60*, 3023–3038.

(42) Ravel, B.; Newville, M. J. *Synchrotron Rad.* **2005**, *12*, 537–541. *Phys. Scr. (Proceedings of the 12th International Conference on X-ray Absorption Fine Structure, Malmö, Sweden, 2003)* **2005**, *T115*, 1007–1010.

(43) Michalowicz, A. *Logiciels pour la chimie*; Société Française de Chimie: Paris, 1991; p 102, and personal communications.

(44) Teo, B. K.; Lee, P. A. *J. Am. Chem. Soc.* **1979**, *101*, 2815–2832.

(45) Zabinsky, S. I.; Rehr, J. J.; Ankudinov, A.; Albers, R. C.; Eller, M. J. *Phys. Rev. B* **1995**, *52*, 2995–3009.

into account the number of fitted parameters. The number of statistically independent data points or maximum number of degrees of freedom in the signal is defined as $N_{\text{idp}} = 2\Delta k \Delta R / \pi$. The k^3 -weighted quality factor is defined as

$$(\Delta\chi)^2/\nu = (1/\nu)(N_{\text{idp}}/N_{\text{pt}}) \sum_k [k^3 \chi_{\text{exp}}(k) - k^3 \chi_{\text{calc}}(k)]^2 / \epsilon^2$$

where $\nu = (N_{\text{idp}} - P)$ is the number of degrees of freedom, P is the number of parameters refined in the fit, N_{pt} is the number of data points in the fitting range, and ϵ is the average statistical measurement error. This experimental error was evaluated with the smoothing method with a low-pass Fourier filtering, using the range above 7 Å in the R -space. The inclusion of extra parameters was statistically validated by a decrease of the quality factor, $(\Delta\chi)^2/\nu$. As recommended, the values of the statistical errors generated in RoundMidnight were multiplied by $[(\Delta\chi)^2/\nu]^{1/2}$, in order to take the systematic errors into account, since the quality factors exceeded one. The error bars thus calculated are given in parentheses after each refined parameter. The scale factor, S_0^2 , was determined by a method already described by B. Ravel,⁴⁷ performing several series of fits on the first shell of the sample mentioned in Figure 13, assuming it characterizes a TiO₄ tetrahedron, and plotting $\sigma_{\text{Ti-O}}^2$ vs S_0^2 for k^1 , k^2 , and k^3 weightings. The value thus found for the scale factor $S_0^2 = 0.89$ was kept constant in all the fits.

Results and Discussion

1. Synthesis of ≡SiO–TiNp₃ on SiO₂–(500) by the Sublimation Method. Silica in general has mainly been characterized by infrared spectroscopy,⁴⁸ which allows to distinguish several different types of surface groups: silanols, coordinated water, and siloxane rings. The concentration of these structures, notably of surface hydroxyl groups, depends on the temperature of dehydroxylation. In order to have a surface uniformly covered with free silanols, not interacting between themselves through hydrogen bondings and thus more reactive for a reaction with an organometallic precursor, the silica surface was dehydroxylated at 500 °C.

Upon grafting TiNp₄, the solid turned pale yellow and neopentane was liberated in the gas phase, which proved that a reaction had taken place. Unreacted starting TiNp₄ was eliminated by heating the silica sample very progressively to 50–60 °C under vacuum, with the silica remaining yellow.

The grafting reaction was followed in situ by infrared spectroscopy. Figure 1 shows the spectrum of the dehydroxylated silica, SiO₂–(500) (Figure 1a) and the spectrum after sublimation of TiNp₄ (Figure 1b) and after desorption of unreacted TiNp₄ (Figure 1c). When TiNp₄ was sublimed onto SiO₂–(500), one notes that the vibration band at 3747 cm^{–1} corresponding to free silanols of initial SiO₂–(500) disappeared completely. A relatively weak band is observed at 3704 cm^{–1} when the titanium complex is grafted. It may correspond to residual silanols weakly interacting with the alkyl groups coordinated to titanium or between themselves through hydrogen bonding. Other new bands appeared at frequencies typical for $\nu(\text{C–H})$ at 2956, 2905, 2867, and 2803 cm^{–1} and $\delta(\text{C–H})$ at 1466, 1394, and 1365 cm^{–1}, vibrational bands characteristic of

(46) Reports of the Standards and Criteria Committee of the International XAFS Society, 2000: http://ixs.iit.edu/subcommittee_reports/sc/.

(47) Ravel, B. *EXAFS Analysis with FEFF and FEFFIT; Part 2: Commentary*, Version 0.001, March 13; 2000; pp 31, 32.

(48) Little, L. H. *Infrared Spectra of Adsorbed Species*; Academic Press: London, 1966.

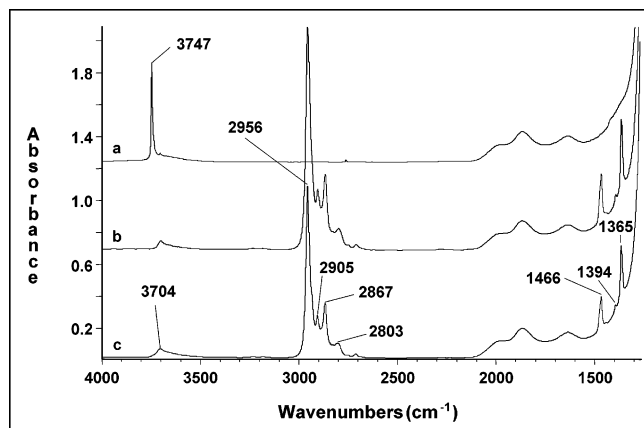


Figure 1. Infrared spectra of the grafting reaction of TiNp_4 onto $\text{SiO}_2-(500)$ by the sublimation method: (a) silica dehydroxylated at $500\text{ }^\circ\text{C}$ for 15 h; (b) after sublimation of TiNp_4 at $50\text{--}60\text{ }^\circ\text{C}$ for 1 h; (c) after treatment under vacuum at $55\text{ }^\circ\text{C}$ for 1 h in order to eliminate the excess of complex (physical adsorption).

neopentyl ligands.⁴⁹ The sublimation of $\text{Zr}(\text{CH}_2\text{tBu})_4$ onto $\text{SiO}_2-(500)$ led to the appearance of similar IR bands (the most intense were reported at 2953, 2864, 1464, 1392, and 1359 cm^{-1}).^{9,50} The desorption of unreacted TiNp_4 was considered to be complete when heating the sample ($55\text{ }^\circ\text{C}$) under vacuum resulted in no significant variation of the intensity of the $\nu(\text{C-H})$ and $\delta(\text{C-H})$ bands. The silanol region of the spectrum was unaffected by this treatment. The irreversible disappearance of the free silanol stretching band and the appearance of $\nu(\text{CH})$ and $\delta(\text{CH})$ bands and of neopentane in the gas phase are further evidences that a chemical reaction had taken place on the silica surface. A sample of the gases given off was analyzed by gas chromatography and shown to contain only neopentane. Further quantification of the alkane products is discussed below.

Titanium elemental analysis was performed on each solid at the end of all reactions. The scale of the preparation was shown to have a profound effect on the total titanium loading: the percentage of grafted titanium was systematically higher on the silica disks than that on larger quantities of silica, typically from 1.4 to 1.8 wt % Ti for thin disks (15–35 mg) and 0.40 to 0.80 wt % Ti for powder samples or thick disks (0.2–0.5 g), as mentioned in Table 1. This difference could be explained by intergranular diffusion problems in the case of larger scale silica preparations. Moreover, one should note a theoretical limit on Ti loading corresponding to total reaction of the free silanols on the silica surface dehydroxylated at $500\text{ }^\circ\text{C}$, about 1.3 OH/nm^2 . If each of these reacts with the titanium complex to form a monopodal $\equiv\text{SiO-TiNp}_3$ surface species, the titanium loading would be 1.8 wt %.

The product was further characterized by ^1H and ^{13}C CP-MAS NMR spectroscopy. Solid state NMR analysis requires a relatively large sample (ca. 200 mg), and as noted above, syntheses on this scale yield relatively low Ti loading, thus complicating NMR analysis. Nevertheless, partial NMR spectra were obtained. ^1H NMR was performed after sublimation of TiNp_4 onto a deuterated silica surface in order to eliminate the peak corresponding to nonreacted silanols (Figure 2a). The peaks at ca. 1.2 and 2.4 ppm are respectively attributed to the methyl

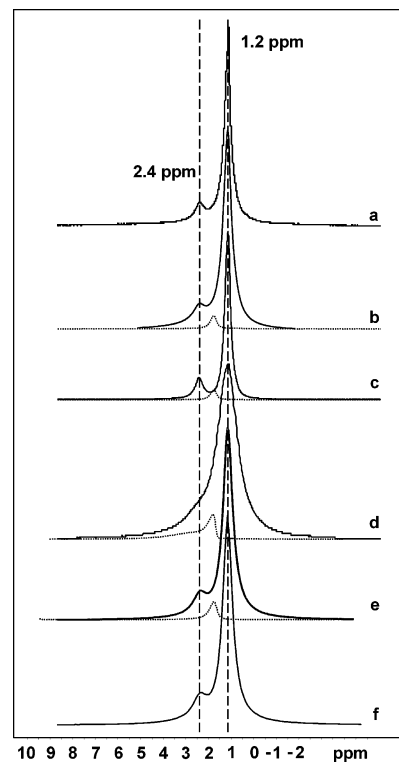


Figure 2. ^1H MAS NMR spectra of the reaction products of TiNp_4 with (a) fully deuterated $\text{SiO}_2-(500)$, preparation by the sublimation method; (b, c, and d) $\text{SiO}_2-(500)$, $\text{SiO}_2-(700)$, and $\text{SiO}_2-(200)$, respectively, preparation by the impregnation method; and (e and f) MCM-41₍₅₀₀₎ and MCM-41₍₂₀₀₎, respectively, preparation by the impregnation method. The spectra of different supports are shown below those of the supported complexes (same scale, dotted line).

and the methylene groups of neopentyl ligands bonded to titanium since these types carbons resonate at 1.18 and 2.22 ppm in the case of the TiNp_4 molecular compound in C_6D_6 .

The ^{13}C CP-MAS NMR spectrum of the grafted species (Figure 3a) shows two signals at ca. 32 and 36 ppm, which can be assigned by comparison with the ^{13}C NMR spectrum of TiNp_4 in C_6D_6 . The signal at 36 ppm is assigned to $-\text{C}(\text{CH}_3)_3$ and the one at 32 ppm to $-\text{C}(\text{CH}_2)_3$, in good agreement with the positions observed in the NMR of TiNp_4 of 37.1 and 33.9 ppm, respectively. The methylene carbon atom that appears at 118.8 ppm for TiNp_4 was expected in the range 120–110 ppm for the supported titanium complex, but it was not detected easily. This phenomenon has also been observed for other supported complexes such as $\equiv\text{SiO-ZrNp}_3$ ⁹ (only the methyl carbon, $-\text{C}(\text{CH}_3)_3$, was first observed at 34 ppm, and a broad signal attributed to the methylene carbon was later observed at ca. 95 ppm on a sample presenting a higher Zr loading⁵⁰) or $\equiv\text{SiO-Ta}(\text{CH}(\text{CH}_3)_3(\text{Np}))_2$ (neither the methylene carbons of the neopentyl nor the carbenic carbon of the neopentylidene ligands was first observed⁵¹) and is related to the fact that the M-CH_2 carbon signal is broader than those of the other carbon atoms of the organic ligand. This is probably due to a lower mobility of these methylenes compared to the rotating methyl groups of tBu and to the heterogeneity of the surface siloxy ligands and also because ^{47}Ti (natural abundance: 7.3%) and ^{49}Ti (natural abundance: 5.5%) are both quadrupolar nuclei, broadening the resonances of the bound carbon atoms. Good signal-to-noise ratios are needed to observe this signal (see below).

(49) Silverstein, R. M.; Bassler, G. C.; Girolami, G. S. In *Spectroscopic Identification of Organic Compounds*, 4th ed.; Wiley-Interscience: New York, (a) p 106, (b) p 206, (c) p 260, (d) 5th ed.; p 242.

(50) Adachi, M.; Nedez, C.; Wang, X. X.; Bayard, F.; Dufaud, V.; Lefebvre, F.; Basset, J. M. *J. Mol. Catal. A: Chem.* **2003**, 204–205, 443–455.

(51) Dufaud, V.; Nicolai, G.; Thivolle-Cazat, J.; Basset, J. M. *J. Am. Chem. Soc.* **1995**, 117, 4288–4294.

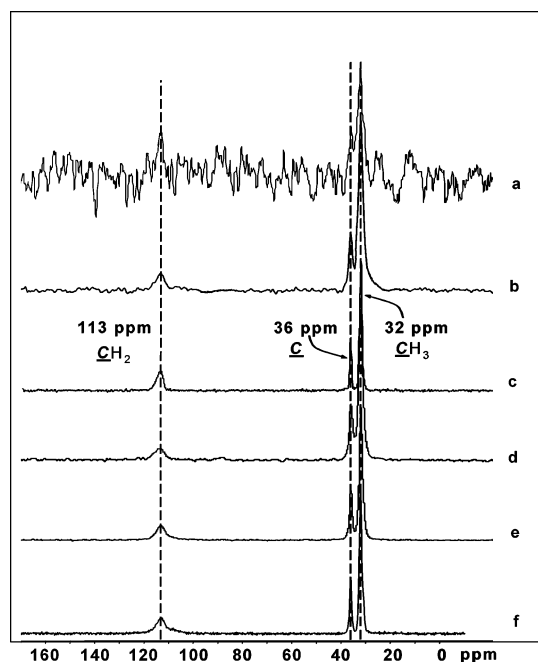


Figure 3. ^{13}C CP-MAS NMR spectra of the reaction products of TiNp_4 with (a) $\text{SiO}_2_{-(500)}$, preparation by the sublimation method (0.5 wt % Ti); (b, c, and d) $\text{SiO}_2_{-(500)}$, $\text{SiO}_2_{-(700)}$, and $\text{SiO}_2_{-(200)}$, respectively, preparation by the impregnation method (1.2, 1.1, and 1.4 wt % Ti, respectively); and (e and f) MCM-41 $_{(500)}$ and MCM-41 $_{(200)}$, respectively, preparation by the impregnation method (3.7 and 4.0 wt % Ti).

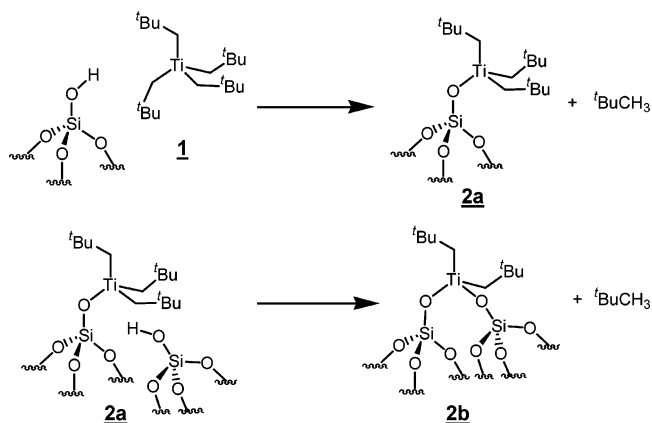
ESR observation of the species revealed that less than 3% of the supported titanium was in the form of metal-based radical Ti(III). We did not try to further characterize this minor species.

The analysis (by gas phase chromatography and mass spectrometry) of the gas evolved during the reaction revealed the presence of only neopentane. Neopentane can be formed either by the grafting reaction or by partial thermal decomposition of TiNp_4 , which may occur under the conditions of sublimation (60 °C). We believe that the thermal decomposition takes place in the break-seal tube (at 60 °C) and not at the silica surface (at 25 °C). So, to distinguish between these two reactions, we performed the grafting of TiNp_4 on a deuterated (>95%) silica. When TiNp_4 was reacted with deuterated silica, neopentane (NpH and NpD) as well as traces of other gases (methane, ethane, propane, isobutane, and isopentane) was liberated.

A key determination is that of the number of neopentyl ligands left on the titanium center after reaction with the silica surface. This determination can be achieved by the quantification of the carbon-to-titanium ratio obtained by elemental analysis. Titanium and carbon elemental analyses of the silica-supported alkyl species were determined for four samples prepared by the sublimation method in a reactor ("large quantities") and gave an average ratio of $\text{C}/\text{Ti} = 13 \pm 2$, which indicates the presence of 2.6 ± 0.4 neopentyl ligands per grafted titanium (theory: 3.0 for $\equiv\text{SiO}-\text{TiNp}_3$).

However the total amount of neopentane given off during the reaction, $(\text{NpH} + \text{NpD})/\text{Ti} = 3.47$, obtained by gas chromatography for an IR pellet of ca. 15 mg (Table 1) does not agree with the elemental analysis. This high value is attributed to the thermal decomposition of TiNp_4 within the break-seal tube. The determination of the ratio NpD/Ti , which is the number of equivalents of neopentane liberated by reaction of TiNp_4 with the deuterated surface silanols, is achieved by determining the NpD/NpH ratio by mass spectroscopy (see

Scheme 1. Grafting Reactions of Tetrakisneopentyl Titanium onto a Silica Surface



Experimental Section for details). The results obtained, 1.04 NpD/Ti for an IR pellet and 1.12 NpD/Ti for a larger amount of powder (Table 1), indicate that the majority of the TiNp_4 had reacted with a single silanol to form $\equiv\text{SiOTiNp}_3$. The variation in the ratio $\text{NpD}/(\text{NpD} + \text{NpH})$ can be attributed to subtle differences in the experimental conditions leading to partial thermal decomposition of TiNp_4 .

The results obtained by elemental analysis and by quantification of gaseous products are consistent with the formation of mainly a monosiloxytrisneopentyl titanium, $\equiv\text{SiOTiNp}_3$ (**2a**). Similar studies have shown the formation of a monosiloxytrisneopentyl zirconium complex, $\equiv\text{SiOZrNp}_3$ in the case of the grafting of ZrNp_4 onto $\text{SiO}_2_{-(500)}$.^{9,50} A small fraction of **2a** possibly reacts with another silanol to give a bisiloxybisneopentyl titanium, **2b** (Scheme 1).

2. Thermal Stability of $\equiv\text{SiO}-\text{TiNp}_3$. Since this species was to be used as the primary supported starting material of all of our subsequent surface titanium syntheses, we were interested in studying the thermal decomposition of $\equiv\text{SiOTiNp}_3$. The complex was heated stepwise from 50 to 400 °C under static vacuum. After 1 h of treatment at each temperature, an infrared spectrum was recorded and the temperature then increased by 25 °C. The appearance of the silica surface changed during this treatment: between 100 and 275 °C, the yellow solid first darkened somewhat. It turned bright yellow above 275 °C. The analysis by gas chromatography of gases evolved during the reaction revealed the presence of neopentane, together with small amounts of methane, ethane, propane, and isobutane.

On the infrared spectrum (Figure 4), it can be observed that the intensity of the $\nu(\text{O}-\text{H})$ vibration bands of silanols increased especially at temperatures above 200 °C. The intensities of the $\nu(\text{C}-\text{H})$ (2956, 2905, 2868, and 2803 cm^{-1}) and $\delta(\text{C}-\text{H})$ (1466, 1394, and 1365 cm^{-1}) vibration bands decrease regularly with increasing temperatures, until their disappearance at 400 °C. The evolution of the alkyl ligands on the silica surface has been quantified by measuring the area of the $\nu(\text{C}-\text{H})$ band remaining for each temperature step. Figure 5 shows the integrated area of the $\nu(\text{CH})$ region (3050–2750 cm^{-1}) at each step of this treatment. The intensity of the signal decreases quite regularly except for a slight discontinuity between 275 and 300 °C. This discontinuity corresponds with the most dramatic color change from brownish yellow to bright yellow.

It can be noted that the supported titanium alkyl complex decomposes easily, even at low temperatures. The results concerning this decomposition can be explained by several phenomena. For temperatures up to 150 °C, only neopentane is liberated and the intensity of the $\nu(\text{C}-\text{H})$ IR bands decreases

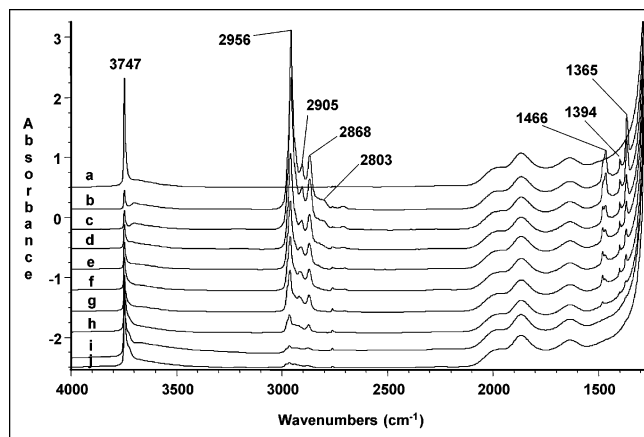


Figure 4. Infrared spectra of the thermolysis reaction of $\equiv\text{SiO-TiNp}_3$ synthesized on $\text{SiO}_{2-(500)}$ by sublimation of TiNp_4 : (a) $\text{SiO}_{2-(500)}$; (b) $\equiv\text{SiO-TiNp}_3$; (c) b after 1 h at 50 °C; (d) c after 1 h at 100 °C; (e) d after 1 h at 150 °C; (f) e after 1 h at 200 °C; (g) f after 1 h at 250 °C; (h) g after 1 h at 300 °C; (i) h after 1 h at 350 °C; (j) i after 1 h at 400 °C.

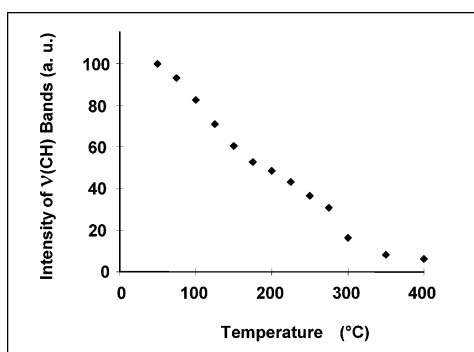
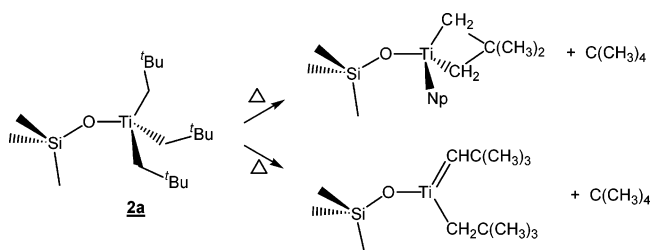


Figure 5. Evolution of the area of the $\nu(\text{C-H})$ bands (3050–2750 cm^{-1} in Figure 4) with temperature.

Scheme 2. Two Possible Pathways for the Thermal Decomposition of **2a** (from ref 52a)



regularly. This could be explained by either α -elimination to a carbene species or γ -elimination to a metallacyclic species (Scheme 2), as proposed for the thermal decomposition of TiNp_4 .⁵² For TiNp_4 decomposition, an intrinsic preference for an α -elimination leading to a titanium carbene was predicted, while for the thermolysis of ZrNp_4 , a γ -elimination would be preferred. However, as in the case of the thermolysis of $(\equiv\text{SiO})_2\text{TiNp}_2$ and $(\equiv\text{SiO})_2\text{ZrNp}_2$ species supported on Aerosil 200,⁵³ no spectral identification of a titanium neopentylidene or metallacyclobutane could be observed by ^{13}C CP-MAS or

(52) (a) Cheon, J.; Rogers, D. M.; Girolami, G. S. *J. Am. Chem. Soc.* **1997**, *119*, 6804–6813 and 6814–6820. (b) Wu, Y.-D.; Peng, Z.-H.; Xue, Z. *J. Am. Chem. Soc.* **1996**, *118*, 9772–9777. (c) Wu, Y.-D.; Peng, Z.-H.; Chan, K. W. K.; Xiaozhan, L.; Tuinman, A. A.; Xue, Z. *Organometallics* **1999**, *18*, 2081–2090.

^1H MAS NMR after thermal treatment of $\equiv\text{SiO-TiNp}_3$ overnight at 85 °C ($\text{NpH/Ti} = 0.8$). The simultaneous formation of lower alkanes, which increases with increasing temperatures, can be explained by the cleavage of the C–C bonds of neopentyl ligands or of neopentane by β -alkyl transfer routes. When the complex is heated at higher temperatures (above 200 °C), the increasing intensity of $\nu(\text{O-H})$ vibration bands of silanols indicates a cleavage of the $\equiv\text{SiO-Ti}$ bonds. Finally, another reaction of the grafted complex occurs at about 275 °C: the brown silica disk becomes suddenly bright yellow and the intensity of the $\nu(\text{C-H})$ vibration bands of the neopentyl ligands decreases. A further study with a temperature-programmed decomposition of the surface species, carried out in situ, under a flow of inert gas, with an on-line GC analysis combined with further IR and MAS NMR analyses of the solid at different steps of the decomposition would be useful in order to understand the mechanism and elucidate the intermediates formed on the silica surface. Nevertheless, this facile decomposition is a factor to be considered in subsequent synthetic protocols developed around this complex.

3. Comparison of the Sublimation and Impregnation Methods. Extension to Other Supports. When the synthesis of the grafted complex is performed in the presence of a solvent (pentane) on $\text{SiO}_{2-(500)}$, the following features are observed (fourth entry in Table 1):

- Most of the hydroxyl groups of the support (60–95%) react with tetrakisneopentyl titanium at room temperature if a slight excess of complex has been introduced (see for example spectrum b in Figure 2, which shows the ^1H MAS NMR spectrum of the reaction product of a nondeuterated silica, $\text{SiO}_{2-(500)}$, with TiNp_4 by impregnation: the signal at 1.8 ppm, characteristic of $\equiv\text{Si-OH}$ groups, is not observed).

- There is no decomposition of the organometallic complex, as all the evolved neopentane is deuterated when the preparation is performed from a deuterated silica.

- As for the sublimation method, there is evolution of only ca. one neopentane molecule per grafted titanium.

As a consequence, we can conclude from these results that the impregnation method allows an easier assessment of the stoichiometry of the reaction by the determination of the formed quantity of neopentane (no decomposition of the starting organometallic complex) and leads to a higher titanium loading than the sublimation method when it is used for large amounts of support (0.5 g). Higher Ti loadings result in easier determinations of the structure of the grafted species, and for example, the ^{13}C CP-MAS NMR spectrum of the grafted species has a better signal-to-noise ratio for similar acquisition times and the signal of the $-\text{CH}_2-$ carbon atom is now well seen at ca. 113 ppm on spectrum b in Figure 3 (118.8 ppm for TiNp_4 in solution).

As the impregnation method is more convenient, gives more reliable results for neopentane evolution, and allows higher Ti loadings, we used it for “large scale” (0.5 g of support) preparations of titanium complexes grafted on the other supports studied. For IR studies (10–20 mg pellets), the sublimation method was used since it led to the saturation of the surface by alkyl titanium grafted complexes and was more convenient. Practically two parameters were studied: (i) the dehydroxylation temperature of silica in order to determine if it has an effect on the structure of the grafted species and (ii) the structure of silica by comparing a flame silica and a mesoporous silica, MCM-41.

(53) Alladin, T.; Beaudoin, M. C.; Scott, S. L. *Inorg. Chim. Acta* **2003**, *345*, 292–298.

Effect of the Dehydroxylation Temperature of the Aerosil Silica on the Structure of the Grafted Organometallic Complex. When the grafting reaction is carried out on $\text{SiO}_{2-(700)}$, the same results as on $\text{SiO}_{2-(500)}$ are obtained: consumption of the hydroxyl groups, all of them in this case, and evolution of only one neopentane molecule per grafted titanium (Table 1). These data, combined with those of NMR spectroscopy (see Figures 2c and 3c), allow us to conclude that $\equiv\text{SiOTiNp}_3$ is formed by reaction of TiNp_4 with the hydroxyl groups of $\text{SiO}_{2-(700)}$. Such a result is not surprising, as the density of hydroxyl groups decreases when the dehydroxylation temperature increases (Table 1). We did not observe on $\text{SiO}_{2-(700)}$ a reaction with the strained $\equiv\text{Si}-\text{O}-\text{Si}\equiv$ siloxane bridges, as reported for Re_2O_7 .⁵⁴ However, the number of strained bridges on a Cab-O-Sil HS-5 silica dehydroxylated at 800 °C is ca. 0.08 per nm^2 ,⁵⁵ and it is expected to be lower for an Aerosil $\text{SiO}_{2-(700)}$, while the number of hydroxyl groups is 0.7 per nm^2 on this support. In the best cases, it would correspond to only ca. 10% of the total amount of grafted complex. The best proof for the opening of a siloxane bridge is to detect by ^{13}C CP-MAS NMR the carbon atom of the neopentyl ligand linked to the silicon atom of the support (at ca. -10 to +10 ppm), but we were unable to observe it, whatever the conditions.

In contrast, when the silica has been dehydroxylated at 200 °C, the situation is completely different: First of all, the amount of evolved neopentane per grafted titanium is higher than 1.0 (Table 1), showing that the reaction of the grafted $\equiv\text{SiO}-\text{TiNp}_3$ complex (ca. 45%) with another silanol group to give a bisiloxo species, $(\equiv\text{SiO})_2\text{TiNp}_2$ (ca. 55%), now becomes predominant. This results in a titanium loading quite similar to that obtained on silica dehydroxylated at 500 °C. The ^1H NMR spectrum (Figure 2d) apparently presents only one very broad signal at ca. 1.2 ppm with a shoulder at 2.4 ppm. This broad signal is in fact the superposition of the resonances of complexes **2a** and **2b** and to those corresponding to residual silanols, $\equiv\text{SiOH}$, free (1.8 ppm) or in interaction with the alkyl groups of the supported complexes. The ^{13}C spectrum (Figure 3d) is very similar to the one obtained for **2a** on $\text{SiO}_{2-(500)}$, except that the band of the methylene group at 113 ppm is slightly wider. It can be emphasized here that we do not distinguish by solid state NMR between the mono- and the bi-grafted titanium complexes. This could be seen, a priori, by an expected upfield variation of the chemical shift of the carbon atom in α -position to Ti (ca. -5 ppm is observed for $\text{Ti}-\text{CH}_2-$ from TiNp_4 [119 ppm] to $\equiv\text{SiO}-\text{TiNp}_3$ [114 ppm on $\text{SiO}_{2-(700)}$], and so -5 ppm would be expected from $\equiv\text{SiO}-\text{TiNp}_3$ to $(\equiv\text{SiO})_2\text{TiNp}_2$ [at ca. 109 ppm]), but the real variation is probably too low, preventing the observation of separated signals.

Reaction of Tetrakisneopentyl Titanium with MCM-41.

It should be first pointed out that the diameter of complex **1**, ca. 12 Å, allows it to circulate within the pores of the MCM-41 support ($\phi = 32 \pm 8$ Å). As above, tetrakisneopentyl titanium reacts with the hydroxyl groups of MCM-41 dehydroxylated at either 200 or 500 °C with evolution of neopentane. As for silica, the data are summarized in Table 1, while Figures 2d and e and 3d and e show the corresponding ^1H and ^{13}C MAS NMR spectra. The elemental analysis data indicate that there is quite the same behavior as on Aerosil silica, i.e., reaction with hydroxyl groups and formation of mono- and bi-grafted titanium species. However, for the same dehydroxylation temperature,

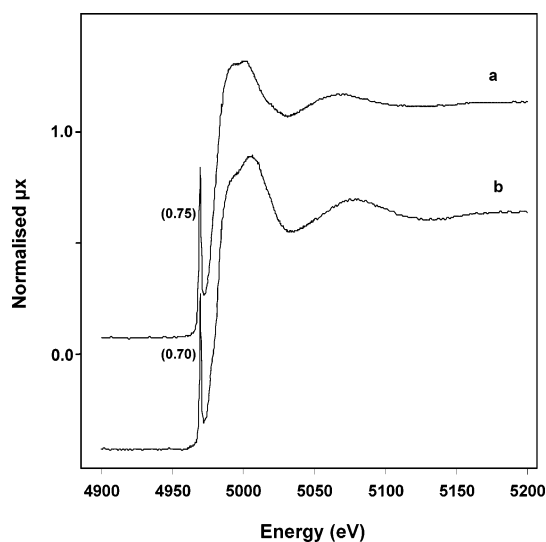


Figure 6. XANES region of Ti K-edge X-ray absorption spectra for (a) $(\equiv\text{SiO})_n\text{TiNp}_{4-n}$ synthesized on $\text{MCM-41}_{(500)}$ and (b) the solid resulting from the reaction of the $(\equiv\text{SiO})_n\text{TiNp}_{4-n}$ complexes ($n = 1$ or 2) synthesized on $\text{MCM-41}_{(500)}$ with *tert*-butyl alcohol. The normalized heights of the pre-edge peaks are indicated in parentheses.

there is formation of more multigrafted species on MCM-41 than on Aerosil silica. Indeed, for several samples of Ti-modified $\text{MCM-41}_{(500)}$, the titanium loading lies between 3.4 and 4.0 wt %, i.e., 0.7 to 0.85 mmol of Ti per gram, and the GC analysis indicates the formation of 1.2 to 1.5 mmol of NpH per gram of support containing the grafted titanium surface species. The average NpH/Ti ratio obtained is 1.65 ± 0.2 neopentane evolved per grafted titanium atom. This value indicates the presence of bisiloxo species since it does not seem to be due to a partial decomposition of the organometallic precursor. There would then remain ca. $4.0 - 1.65 = 2.35$ neopentyl ligands per grafted titanium atom. The carbon loading of the samples lies in the range 11–12.5 wt %, which gives an average C/Ti ratio of 12, i.e., an average of 2.4 remaining neopentyl ligands per grafted titanium, and agrees with the value deduced from the gas evolution. This value is also confirmed by the hydrolysis of the surface fragments, which gives an average of 2.3 NpH released per grafted Ti. These results are thus consistent with the formation of ca. 35% of $\equiv\text{SiO}-\text{TiNp}_3$ (**2a**) and 65% of $(\equiv\text{SiO})_2\text{TiNp}_2$ (**2b**) as the major surface species on $\text{MCM-41}_{(500)}$, while it is practically not observed on $\text{SiO}_{2-(500)}$. Such a behavior had been previously observed for zirconium complexes: A more important proportion of multigrafted species was formed on the MCM-41 surface than on the Aerosil silica surface.⁵⁶ This can be related to a different repartition of the silanols between Aerosil silica and the structured MCM-41, although they present similar average silanol densities. It could also be that the OH groups of MCM-41 present a different kind of acidity, leading to a different reactivity and to a different structure of the grafted Ti complex. Observation of the grafted species by ESR revealed that less than 2% of the supported titanium is present in the form of a metal-based Ti^{III} radical.

The NMR spectra (parts e and f in Figures 2 and 3) of the supported species do not show a great difference from those obtained on silica, if one excepts a higher signal-to-noise ratio for the same acquisition times (the titanium loading being increased by a factor 3). Here again the mono- and bi-grafted

(54) Scott, S. L.; Basset, J. M. *J. Am. Chem. Soc.* **1994**, *116*, 12069–12070.

(55) Morrow, B. A.; Cody, I. A. *J. Phys. Chem.* **1976**, *80*, 1998–2004.

(56) Wang, X. X.; Veyre, L.; Lefebvre, F.; Patarin, J.; Basset, J. M. *Micropor. Mesopor. Mater.* **2003**, *66*, 169–179.

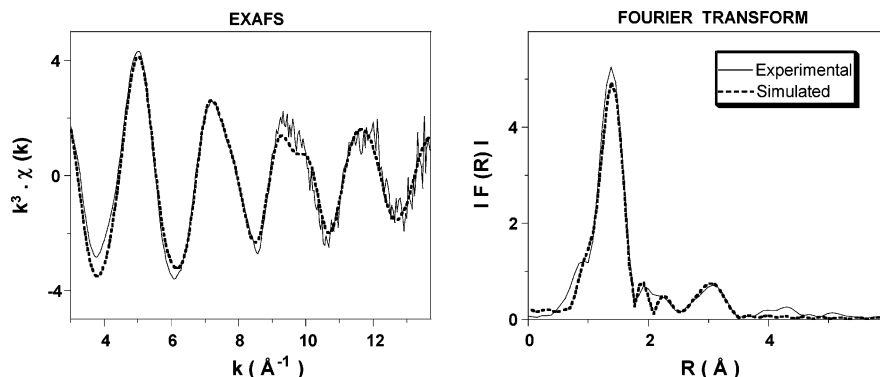


Figure 7. Ti K-edge k^3 -weighted EXAFS (left) and Fourier transform (right) of $(\equiv\text{SiO})_n\text{TiNp}_{4-n}$ complexes synthesized on $\text{MCM-41}_{(500)}$. Solid lines: experimental. Dotted lines: spherical wave theory.

titanium complexes could not be clearly distinguished by NMR (comparison of spectrum 3c for **2a** supported on $\text{SiO}_2-(700)$ with spectrum 3f for **2b** on $\text{MCM-41}_{(200)}$).

The Ti-K XANES region of the X-ray absorption spectrum of the solid obtained after the grafting of TiNp_4 onto $\text{MCM-41}_{(500)}$ is shown in Figure 6a. A sharp and intense pre-edge peak is observed at 4969.6 ± 0.3 eV with a normalized height of 0.75 and a half-height width of 2.1 eV. Although the 1s to 3d transition is forbidden, an overlap of the 4p and 3d orbitals of Ti allows the appearance of a pre-edge peak. The symmetry of the complex (formation of molecular orbitals mixing Ti 3d and 4p with the orbitals of the ligands) can make this transition partly allowed and visible. This is in particular the case when Ti(IV) is in a tetrahedral or quasi tetrahedral coordination, as in $\text{Ti}(\text{O}^i\text{Am})_4$,⁵⁷ $\text{Ti}(\text{OSiPh}_3)_4$, and $\text{Ti}(\text{OGePh}_3)_4$ ⁵⁸ molecular compounds, in several titanium oxides,⁴¹ or in TS-1,⁵⁹ where an intense pre-edge peak is observed. Farges et al. analyzed various Ti model compounds by XANES⁴¹ and showed that those composed of four-coordinated Ti(IV) present the most intense pre-edge peaks in the energy range 4969.3–4970 eV with a maximum intensity in the range 0.67–1.03, while the position in energy of the pre-edge peak for five-coordinated Ti compounds is above 4970.5 eV with an intensity lower than 0.73 (for six-coordinated Ti compounds: position above 4971.1 eV for the main pre-edge peak with an intensity below 0.32). By analogy with this study, the position and the strong intensity of the pre-edge peak observed for the solid obtained after the grafting of TiNp_4 onto $\text{MCM-41}_{(500)}$ may be considered as a good indication that titanium is present as four-coordinated Ti(IV) in the material.

Figure 7 shows the experimental and fitted EXAFS signals obtained for the $(\equiv\text{Si-O})_n\text{Ti}(\text{Np})_{4-n}$ complexes supported on $\text{MCM-41}_{(500)}$. In the fit, the sum of the bound carbon and oxygen neighbors was kept constant at 4 ($N_{\text{O}} + N_{\text{C}} = 4.0$), assuming from the XANES results that titanium is four-coordinated. The best fit corresponds to 1.7 oxygen atoms at 1.81 Å and 2.3 carbon atoms at 2.01 Å coordinated to titanium (with a k^1 weighting the results of the fit do not change much: 1.5(4) O at 1.82(2) Å, $\sigma_{\text{Ti-O}^2} = 0.0014(8)$ Å² and 2.5 C at 2.03(3) Å,

$\sigma_{\text{Ti-C}^2} = 0.008(3)$ Å²). These distances are in good agreement with values obtained from crystallographic data for four-coordinated Ti–OSi≡ complexes (1.786 to 1.828 Å for bis-(heptakis(cyclohexyl)(trimethylsiloxy)heptasilasesquioxane)-titanium toluene solvate;³⁵ 1.782 and 1.798 Å for $\text{Ti}(\text{OSiPh}_3)_4$;⁶⁰ and 1.843 Å for $[\text{Cp}_2\text{ClTi-O-SiMe}_2(\text{CH}_2\text{Cl})]^{61}$) and for Ti– $\text{CH}_2\text{C}(\text{Me})_3$ (2.01 to 2.04 Å for the three symmetry independent but chemically equivalent molecules in the crystal structure of $(\text{Me}_3\text{Si})_3\text{SiTi}(\text{CH}_2\text{CMe}_3)_3$;⁶²). Three additional constrained shells were tentatively added to improve the fit, one with carbon at 3.40 Å, corresponding to the nonbonding quaternary carbon atoms of the neopentyl ligands (this distance lies in the 3.30–3.42 Å range obtained for similar Ti···C distances found in $(\text{Me}_3\text{Si})_3\text{SiTi}(\text{CH}_2\text{CMe}_3)_3$;⁶²), another shell with silicon at 3.42 Å, corresponding to the silicon atoms of $\equiv\text{SiO-Ti}$ moieties (this distance lies in the 3.25–3.50 Å range obtained by DFT calculations for Ti···Si distances determined in $\equiv\text{SiO-Ti}$ moieties⁶³), and the last shell with one oxygen at ca. 3.0 Å, attributed to a surface siloxane, as previously proposed¹¹ for a silica-supported zirconium hydride. The inclusion of these extra parameters decreased the quality factor, $(\Delta\chi)^2/\nu$, from 1.45 ($\nu = 14$) for the two-shell model to 1.35 ($\nu = 11$). The fits including three or four shells even with many constraints all presented a higher quality factor than the fit with only two shells (O + C bound atoms), as well as fits considering five shells with less constraints. The EXAFS-derived parameters are collected in Table 2.

Similarly, the analysis by Corker et al. of the Zr K-edge EXAFS of $\equiv\text{SiO-Zr}(\text{CH}_2\text{Bu})_3$ grafted onto an Aerosil $\text{SiO}_2-(500)$ gave a first coordination sphere of Zr with one O atom at 1.96 Å ($\sigma_{\text{Zr-O}^2} = 0.0033$ Å²) and three C atoms at 2.22 Å ($\sigma_{\text{Zr-C}^2} = 0.0081$ Å²), and an additional shell at 3.42 Å could be tentatively assigned to three nonbonding neopentyl C atoms ($\sigma_{\text{Zr-C}^2} = 0.013$ Å²), although the quality of the data limited the precision of this distant shell.¹¹ The distances reported were also consistent with corresponding distances obtained from X-ray crystallography studies for analogous zirconium molecular complexes.

In our EXAFS analysis of the titanium alkyl complexes supported on $\text{MCM-41}_{(500)}$, systematic errors exist, as evidenced by the value of the quality factor, which slightly exceeds 1.⁴⁶ One of these errors is identifiable since the data concern the

(57) Babonneau, F.; Doeuff, S.; Leautic, A.; Sanchez, C.; Cartier, C.; Verdager, M. *Inorg. Chem.* **1988**, *27*, 3166–3172.

(58) (a) Gleeson, D.; Sankar, G.; Catlow, R.; Thomas, J. M.; Spano, G.; Bordiga, S.; Zecchina, A.; Lamberti, C. *Phys. Chem. Chem. Phys.* **2000**, *2*, 4812–4817. (b) Thomas, J. M.; Sankar, G. *Acc. Chem. Res.* **2001**, *34*, 571–581.

(59) (a) Bordiga, S.; Coluccia, S.; Lamberti, C.; Marchese, L.; Zecchina, A.; Boscherini, F.; Buffa, F.; Genoni, F.; Leofanti, G.; Petrini, G.; Vlaic, G. *J. Phys. Chem.* **1994**, *98*, 4125–4132. (b) Bordiga, S.; Damin, A.; Bonino, F.; Zecchina, A.; Spano, G.; Rivetti, F.; Bolis, V.; Prestipino, C.; Lamberti, C. *J. Phys. Chem. B* **2002**, *106*, 9882–9905.

(60) Johnson, B. F. G.; Klunduk, M. C.; Martin, C. M.; Sankar, G.; Teate, S. J.; Thomas, J. M. *J. Organomet. Chem.* **2000**, *596*, 221–225.

(61) Enders, M.; Fink, J.; Mailland, V.; Pritzkow, H. *Z. Anorg. Allg. Chem.* **2001**, *627*, 2281–2288.

(62) McAlexander, L. H.; Hung, M.; Li, L.; Diminnie, J. B.; Xue, Z.; Yap, G. P. A.; Rheingold, A. L. *Organometallics* **1996**, *15*, 5231–5235.

(63) Barker, C. M.; Gleeson, D.; Kaltsoyannis, N.; Catlow, C. R. A.; Sankar, G.; Thomas, J. M. *Phys. Chem. Chem. Phys.* **2002**, *4*, 1228–1240.

Table 2. Ti K-Edge EXAFS-Derived Structural Parameters (k^3 Weighting) for $(\equiv\text{SiO})_n\text{TiNp}_{4-n}$ Species, Synthesized on MCM-41₍₅₀₀₎, and for the $(\equiv\text{Si}-\text{O})_n\text{Ti}(\text{O}^t\text{Bu})_{4-n}$ Species, Obtained after Reaction of **2a and **2b** with *tert*-Butyl Alcohol (single scattering theory; values in parentheses represent the errors generated in RoundMidnight)**

scatterer	coordination number	distance from Ti (Å)	D.W. factor (σ^2 , Å ²)
$(\equiv\text{Si}-\text{O})_n\text{Ti}(\text{Np})_{4-n}$ Species ^a			
Ti–O	1.7(4)	1.81(1)	0.0022(11)
Ti–C	2.3 ^b	2.01(3)	0.0062(23)
Ti···O′Si ₂	1	2.96(5)	0.0062 ^b
Ti···C	2.3 ^b	3.40(6)	0.0062 ^b
Ti···Si	1.7 ^b	3.42(5)	0.0062 ^b
$(\equiv\text{Si}-\text{O})_n\text{Ti}(\text{O}^t\text{Bu})_{4-n}$ Species ^c			
Ti–O	4.0	1.80(1)	0.0047(6)
Ti···C	2.7(5)	2.98(3)	0.0058(27)
Ti···Si	1.3 ^d	3.46(4)	0.0058 ^d

^a Fit residue: $\rho = 7\%$ ($\Delta k = 3.1\text{--}13.7 \text{ \AA}^{-1}$, $\Delta R = 0.6\text{--}3.6 \text{ \AA}$); energy shift: $\Delta E_0 = -0.6 \pm 1.2 \text{ eV}$, the same for all shells; overall scale factor: $S_0^2 = 0.89$; number of parameters fitted: $P = 9$; number of degrees of freedom in the fit: $\nu = 11$; quality factor of the fit: $(\Delta\chi)^2/\nu = 1.35$. ^b Shell constrained: $N_{\text{O}} + N_{\text{C}} = 4.0$; $N_{\text{C}} = N_{\text{C}}$; $N_{\text{Si}} = N_{\text{O}}$; $\sigma_{\text{Si}}^2 = \sigma_{\text{C}}^2 = \sigma_{\text{O}}^2 = \sigma_{\text{C}}^2$. ^c Fit residue: $\rho = 4.5\%$ ($\Delta k = 3.2\text{--}13.7 \text{ \AA}^{-1}$, $\Delta R = 0.5\text{--}3.6 \text{ \AA}$); energy shift: $\Delta E_0 = -1.2 \pm 1 \text{ eV}$, the same for all shells; overall scale factor: $S_0^2 = 0.89$ (fitted on the filter of the first peak in the FT); number of parameters fitted: $P = 7$; number of degrees of freedom in the fit: $\nu = 13$; quality factor of the fit: $(\Delta\chi)^2/\nu = 1.3$. ^d Shell constrained: $N_{\text{C}} + N_{\text{Si}} = 4.0$; $\sigma_{\text{Si}}^2 = \sigma_{\text{C}}^2$.

presence of two supported complexes, **2a** and **2b**, while for the fit the formulation of an “average single-site model” was considered with in particular only one distance per type of neighbor. However this model seems to describe correctly the mixture of the two sites as shown below:

(i) No important differences are expected between the Ti–C or Ti–O bond distances of these two Ti(–O)(–C)₃ (**2a**) and Ti(–O)₂(–C)₂ (**2b**) type complexes, as is the case for the two following complexes, both presenting benzyl ligands. For (Ph₂CH₂)₃Ti–O–Ti(CH₂Ph)₃,⁶⁴ with Ti(–O)(–C)₃ type centers, and (2,6-Ph₂C₆H₃O)₂Ti(CH₂Ph)₂,⁶⁵ a Ti(–O)₂(–C)₂ type complex, the amplitudes of the bond distance distributions are lower than 0.029 Å for Ti–C (2.076(9)–2.091(5) Å range) and 0.020 Å for Ti–O (1.784(3)–1.798(3) Å range), while there are two very different types of oxygenated ligands (μ -oxo and aryloxy) in these compounds. Similarly, in the case of (2,6-Ph₂C₆H₃O)₂–Ti(CH₃)₂ and (2,6-Ph₂C₆H₃O)₃Ti(CH₃), a Ti(–O)₂(–C)₂ and a Ti(–O)₃(–C) type complex, respectively, both presenting the same alkyl and oxygenated ligands,⁶⁵ the amplitudes of the bond distance distributions are lower than 0.024 Å for Ti–C (2.052(2)–2.070(4) Å range) and 0.010 Å for Ti–O (1.791(1)–1.798(2) Å range). The amplitudes observed for the Ti–C or Ti–O bond distances in these complexes are rather small and lower than the error bars determined by our EXAFS analysis ($2 \times 0.03 = 0.06 \text{ \AA}$ and $2 \times 0.01 = 0.02 \text{ \AA}$ for the Ti–C and Ti–O distances, respectively).

(ii) Moreover it can be pointed out that the “average coordination numbers” found by EXAFS, $1.7 \pm 0.4 \text{ O/Ti}$ and $2.3 \pm 0.4 \text{ C/Ti}$, are roughly in good agreement with the formulations obtained from chemical analyses, gas evolution, and hydrolysis of the sample, $1.65 \pm 0.2 \text{ O/Ti}$ and $2.35 \pm 0.2 \text{ C/Ti}$.

(iii) Furthermore the values of the Debye–Waller factors (σ^2 , Å²), which are 0.0022 Å² ($\sigma_{\text{Ti}-\text{O}}^2$) and 0.0062 Å², seem reasonable although this last value may seem slightly high for

the $\sigma_{\text{Ti}-\text{C}}^2$ in the first coordination sphere of Ti, if compared with a crystalline compound such as Ti(OSiPh₃)₄,^{58–a} where $2\sigma_{\text{Ti}-\text{O}}^2$ values of 0.007 Å² were found. However for grafted complexes, higher values are often found for the Debye–Waller factors, as shown in the case of $\equiv\text{SiO}-\text{Zr}(\text{CH}_2^t\text{Bu})_3$ mentioned above, and may be indicative of more than thermal disorder. For instance in the case of the direct grafting of TiCp₂Cl₂ on a MCM-41 support, σ^2 values were found in the range 0.008–0.010 Å² in the first coordination sphere of the anchored complex, while they were in the range 0.003–0.005 Å² in the free or physisorbed complex.³¹ Relatively high Debye–Waller factors may be due to structural disorders, since there is a heterogeneity in the distribution and the orientation of the silanols on the surface of the support, which gives rise to complexes with different types of siloxy ligands. In addition, in the case of complexes **2a** and **2b** supported on MCM-41₍₅₀₀₎, the consideration of an average single-site model with in particular only one distance per type of neighbor may also slightly spread the distribution of these distances, as seen above in (i).

In conclusion, considering the bond distances, the coordination numbers, and the Debye–Waller factors obtained from this fit, presenting a quality factor $(\Delta\chi)^2/\nu = 1.35$ with a degree of freedom $\nu = 11$, it seems that an average single-site model is a reasonable choice and describes correctly a mixture of the two sites.

To summarize, the XAS data are also consistent with the presence of four-coordinated Ti complexes supported on MCM-41₍₅₀₀₎, ($\equiv\text{SiO})_2\text{TiNp}_2$ (**2b**) as a major species and $\equiv\text{SiO}-\text{TiNp}_3$ (**2a**).

In conclusion of this part, it appears that sublimation and impregnation preparation methods lead to the same surface species, but the impregnation method has the great advantage of avoiding partial decomposition of the starting organometallic complex. Comparison of Aerosil silica and MCM-41 shows that MCM-41 has a greater tendency to form multigrafted species, while the average silanol densities are relatively similar on both supports. A shorter distance between the silanol OH groups of MCM-41 and a different kind of acidity of the OH groups between Aerosil silica and MCM-41 may be responsible for this behavior.

4. Hydrolysis of the $(\equiv\text{Si}-\text{O})_n\text{Ti}(\text{Np})_{4-n}$ Species ($n = 1, 2$). The reaction of silica-supported monosiloxytrisneopentyl titanium with water was followed by infrared spectroscopy and the analysis of the gas phase performed by gas chromatography. The titanium surface complex was exposed to an excess of H₂O (18–31 Torr at 20–30 °C), leading to an immediate reaction at room temperature as the yellow solid became white. The reaction was followed by in situ IR spectroscopy (Figure 8).

The $\nu(\text{C}-\text{H})$ vibration bands characteristic of neopentyl ligands disappeared immediately and completely. Broad vibration bands at 3674 and 3543 cm^{–1} are observed. They cannot be assigned to the stretching vibration of H₂O, because there is no corresponding deformation band at ca. 1640 cm^{–1}. They almost certainly correspond to the O–H stretching mode of H-bonded surface silanols and probably $\equiv\text{Ti}-\text{OH}$ groups. The increase of the band at 3744 cm^{–1} indicates that free silanol groups are recovered, due to the cleavage of siloxane bridges $\equiv\text{Si}-\text{O}-\text{Si}\equiv$ (rehydration of silica) and maybe of $\equiv\text{Si}-\text{O}-\text{Ti}\equiv$ bonds.

Gas phase analysis showed the liberation of neopentane as the only volatile organic product. The amount of NpH evolved was quantified by gas chromatography and compared to the relevant titanium microanalysis. The ratio NpH evolved/Ti

(64) Stoeckli-Evans, H. *Helv. Chim. Acta* **1974**, *57*, 684–689.

(65) Thorn, M. G.; Etheridge, Z. C.; Fanwick, P. E.; Rothwell, I. P. *J. Organomet. Chem.* **1999**, *591*, 148–162.

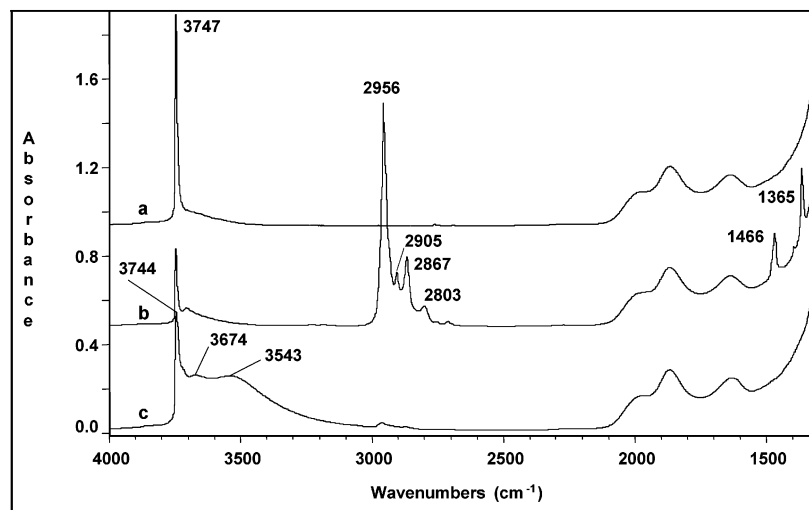


Figure 8. Hydrolysis reaction of $\equiv\text{SiO}-\text{TiNp}_3$: (a) silica dehydroxylated at 500 °C; (b) after reaction with TiNp_4 ; (c) b after reaction with H_2O and thermal treatment at 70 °C under vacuum for 3 h in the presence of a cold trap at 77 K.

obtained by hydrolysis of the grafted titanium alkyl was repeatedly about 3, in agreement with the formula $\equiv\text{SiO}-\text{TiNp}_3$ for the surface alkyl complex supported on $\text{SiO}_2-(500)$.

The reaction was repeated using D_2O rather than H_2O with the objective of demonstrating that there was no carbene species present, neither $\text{Np}_2\text{Ti}(\text{=CHC}(\text{CH}_3)_3)$ resulting from a thermal degradation of TiNp_4 nor $(\equiv\text{SiO})\text{TiNp}(\text{=CHC}(\text{CH}_3)_3)$ formed during the grafting reaction on the silica surface. The reaction was followed by infrared spectroscopy, and the liberated gases were determined by GC-MS. Analysis confirmed that almost all the surface neopentyl groups were consumed and that neopentane- d_1 was the only gaseous product of deuterolysis. This was in agreement with the absence of any carbene species on the surface.

From our study on the hydrolysis of $(\equiv\text{SiO})\text{TiNp}_3$, no formulation could be proposed for the resulting titanium species, which were not characterized in detail. However the results confirmed the structure proposed for the $\text{SiO}_2-(500)$ -supported alkyl complex **2a**, as 3 equiv of neopentane were liberated per grafted titanium. Finally, the deuterolysis of the complex showed there was no carbene species on the silica surface.

5. Reaction of the $(\equiv\text{Si}-\text{O})_n\text{Ti}(\text{Np})_{4-n}$ Species ($n = 1, 2$) with Alcohols. We were particularly interested in the study of the reaction of the monosiloxytrisneopentyl titanium with alcohols in order to obtain new surface species, presumably of the form $(\equiv\text{SiOTi}(\text{OR})_3)$ (**3a_{OR}**), one of our ultimate target species for oxidation catalysis. Methanol, ethanol, and *tert*-butyl alcohol were chosen, to provide very different steric environments at titanium. The reactions were followed by infrared spectroscopy, GC, solid state NMR, and elemental analysis. The reaction was studied for Ti complexes supported on both Aerosil $\text{SiO}_2-(500)$ and MCM-41 $_{(500)}$. Whatever the support, the results were identical, only the amount of evolved neopentane being different.

Reaction of $(\equiv\text{SiO})\text{TiNp}_3$ with Methanol. When $(\equiv\text{SiO})\text{TiNp}_3$ prepared on $\text{SiO}_2-(500)$ was exposed to methanol vapor, the yellow silica disk turned immediately to white. Infrared spectroscopy showed that the $\nu(\text{C}-\text{H})$ and $\delta(\text{C}-\text{H})$ vibration bands characteristic of neopentyl ligands disappeared after reaction with methanol and were replaced by new $\nu(\text{C}-\text{H})$ (2957, 2928, 2896, 2854, and 2827 cm^{-1}) and $\delta(\text{C}-\text{H})$ (1481, 1463, 1437, 1397, and 1367 cm^{-1}) bands, which can be attributed to methoxy ligands.

The quantification of the gas phase revealed neopentane as the only gaseous product of the reaction, and for a sample prepared on a larger scale, comparison to the titanium microanalysis gave a ratio NpH/Ti of 3, as expected for a quantitative exchange of the neopentyl of **2a** by methoxy ligands. The results of the titanium and carbon elemental analyses of this last sample were 1.41 wt % Ti and 1.10 wt % C, corresponding to a ratio $\text{C}/\text{Ti} = 3.1$, which is that expected for three methoxy ligands per grafted titanium in a $\equiv\text{SiO}-\text{Ti}(\text{OME})_3$ complex, considering the precision of the chemical analyses.

The XPS spectrum of the complex showed notably a broadened peak at 460.6 eV (measured vs the C 1s peak reference at 285.0 eV) attributed to Ti 2p $_{3/2}$. This energy is higher than that normally associated with tetrahedral Ti(IV) (e.g., 459.8 eV for TS-1), and the XPS spectrum of the silica blank showed some titanium present in the support (bond energy at 461.9 eV, ca. 0.5 at. % Ti), which might contribute to the shift to higher energy and certainly to the peak width. The higher energy might also be an effect of the organic ligands of the complex. The XPS spectrum does not completely exclude the presence of a small contribution of octahedral Ti(IV) (bond energy at 458.3 eV for anatase); however, no obvious shoulder on the low-energy side of the peak is observed on the spectrum.

The diffuse reflectance (DR) UV-vis spectrum of this supported complex vs silica blank reference showed two peaks at 216 and 258 nm. UV-vis spectroscopy has been extensively used to characterize the titanium phases present in titanosilicates such as TS-1,^{59,66-69} Ti-MCM-41,^{70,71} and Ti-SBA15,^{32,72} in

(66) Boccuti, M. R.; Rao, K. M.; Zecchina, A.; Leofanti, G.; Petrini, G. *Stud. Surf. Sci. Catal.* **1989**, *48*, 133-144.

(67) Zecchina, A.; Spoto, G.; Bordiga, S.; Ferrero, A.; Petrini, G.; Leofanti, G.; Padovan, M. *Stud. Surf. Sci. Catal.* **1991**, *65*, 251-258.

(68) Le Noc, L.; Trong On, D.; Solomykina, S.; Echchahed, B.; B eland, F.; Cartier dit Moulin, C.; Bonneviot, L. *Stud. Surf. Sci. Catal.* **1996**, *101*, 611-620.

(69) Duprey, E.; Beauvier, P.; Springuel-Huet, M. A.; Bozon-Verduraz, F.; Fraissard, J.; Manoli, J. M.; Br egeault, J. M. *J. Catal.* **1997**, *165*, 22-32.

(70) Blasco, T.; Corma, A.; Navarro, M. T.; P erez Pariente, J. *J. Catal.* **1995**, *156*, 65-74.

(71) Marchese, L.; Mashmeyer, T.; Gianotti, E.; Coluccia, S.; Thomas, J. M. *J. Phys. Chem. B* **1997**, *101*, 8836-8838.

(72) Chiker, F.; Nogier, J. P.; Launay, F.; Bonardet, J. L. *Appl. Catal. A* **2003**, *243*, 309-321. Chiker, F.; Nogier, J. P.; Launay, F.; Bonardet, J. L. *Appl. Catal. A* **2004**, *259*, 153-162.

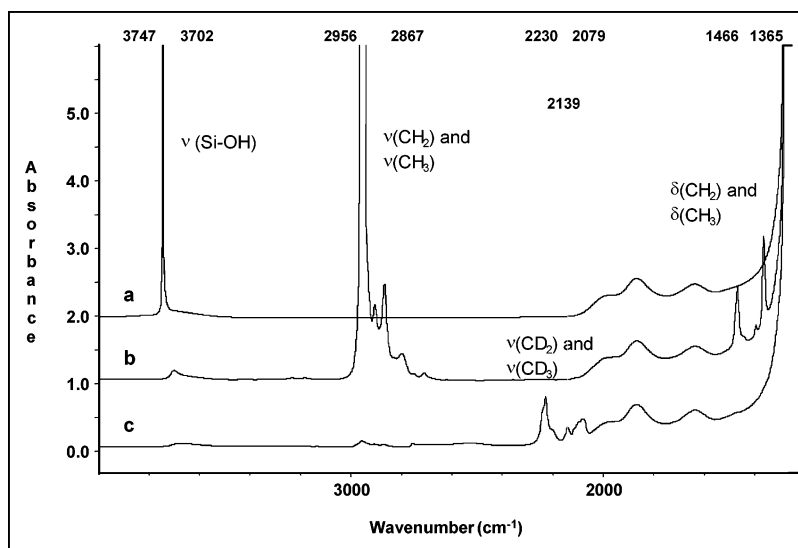


Figure 9. Sublimation of TiNp_4 on $\text{SiO}_2-(500)$ followed by an ethanolysis of the supported complexes with ethanol- d_6 : (a) dehydroxylated silica; (b) after sublimation; (c) after ethanolysis and thermal treatment at 80 °C under vacuum for 3 h in the presence of a cold trap at 77 K, to remove physisorbed ethanol.

amorphous titania–silica mixed oxides,⁷³ or in faujasites⁷⁴ and titanium molecular complexes such as titanium silasesquioxane.³⁵ The DR–UV–vis spectrum of the solid obtained after reaction of **2a** with methanol showed the absence of TiO_2 particles in the material since in their presence the absorption edge is usually observed at 350–370 nm with a shoulder at ca. 320 nm.⁶⁷ In the case of a TS-1 titanium-silicalite, an electronic absorption has been attributed to a charge transfer between the oxide ions of the lattice, hydroxyl groups, and water molecules bonded to titanium and an empty d-orbital of Ti(IV) .⁶⁶ The position of this band is at ca. 208 nm for tetrahedral Ti(IV) centers and is reversibly shifted to ca. 240 nm upon adsorption of water, due to a higher coordination state of the Ti(IV) centers. For partly hydrated amorphous titania–silica mixed oxides with Ti contents lower than 9 mol %, a bimodal DRS signal was observed; one maximum at ca. 200–220 nm was similarly associated with isolated, tetrahedral Ti(IV) species in a silica matrix and the other at ca. 250–280 nm with Ti(IV) centers in a coordination higher than tetrahedral due to the coordination of water or residual alcohol.⁷³ This last signal was removed under dry conditions, after a calcination at 573 K. The energy of a LMCT band in a coordination complex does not generally demonstrate or refute its coordination number; however by analogy with the studies reported above, the peak observed at 216 nm in the sample may be considered as characteristic of isolated tetrahedral titanium(IV), whereas the band at 258 nm would indicate the presence of some Ti(IV) in a higher coordination number. It can then be suggested that there was some water or methanol coordinated on the Ti(IV) centers, resulting in a formula such as $\equiv\text{SiOTi}(\text{OCH}_3)_3 \cdot (\text{H}_2\text{O})_x \cdot (\text{CH}_3\text{-OH})_y$. However the results of the chemical analyses indicated above do not seem to agree with the presence of much methanol coordinated to titanium ($y \approx 0$); it then seems that mainly water was interacting with the $\equiv\text{SiOTi}(\text{OCH}_3)_3$ complex analyzed by UV–vis spectroscopy. The presence of this water seems to be due to the short exposure of the sample to ambient air (10 min) before and during the recording of the UV–vis spectrum.

(73) Klein, S.; Weckhuysen, B. M.; Martens, J. A.; Maier, W. F.; Jacobs, P. A. *J. Catal.* **1996**, *163*, 489–491.

(74) Klaas, J.; Schulz-Ekloff, G.; Jaeger, N. *J. Phys. Chem.* **1997**, *101*, 1305–1311.

On the ^1H MAS NMR spectrum of the complex, three significant peaks could be resolved at 3.4, 1.8, and 0.8 ppm, the first one being the most intense. The peak at 1.8 ppm can be reasonably attributed to surface silanol groups, while that at 0.8 ppm may correspond to a few unreacted alkyl groups on titanium. Methanol in solution gives ^1H NMR signals at 3.31 (CH_3) and 4.79 (OH) ppm. The most intense peak (3.4 ppm) could then be attributed to the protons of methoxide ligands bonded on titanium.

Thus from all these results we conclude that the reaction has produced silica-supported monosiloxytrimethoxy titanium species, $\equiv\text{SiO-Ti}(\text{OMe})_3$ (**3a_{OMe}**).

Reaction of $\equiv\text{SiO-TiNp}_3$ with Ethanol. When the alkyl complex **2a** was exposed to ethanol vapor at room temperature, a reaction occurred immediately, as shown by the color change of the sample, from yellow to white. In situ infrared studies were carried out on the reaction between $\equiv\text{SiOTiNp}_3$ and perdeuterated ethanol. The use of this reagent allows the differentiation between newly formed ethoxy and initial neopentyl bands. The spectra are shown in Figure 9. After introduction of ethanol, the $\nu(\text{C-H})$ and $\delta(\text{C-H})$ bands at 2956, 2905, 2867, and 2803 cm^{-1} and 1466 and 1365 cm^{-1} , respectively, disappear, while new bands appear at 2230, 2139, and 2079 cm^{-1} corresponding to $\nu(\text{C-D})$ bands of the ethoxy moiety.

Analysis of the evolved gas phase for a sample prepared from **2a** and ethanol on a larger scale showed that it was composed of only neopentane, in a 3/1 ratio compared to the amount of grafted titanium ($\text{NpH/Ti} = 3.0$). The microanalysis showed the presence of a small excess of carbon ($\text{C/Ti} = 6.8$ instead of 6 in the presumed $\equiv\text{SiO-Ti}(\text{OEt})_3$ complex), which could be attributed to the presence of $\equiv\text{Si-OEt}$ surface groups⁷⁵ or to a few ethanol molecules (less than 0.4 EtOH per Ti) H-bonded to residual silanols or coordinated to Ti.

The two signals observed at 1.1 and 3.8 ppm on the ^1H spectrum of the surface complex (Figure 10A) are respectively attributed to the protons of methyl and methylene of ethoxy groups. The ^{13}C CP-MAS NMR spectrum displays three peaks at 73, 59, and 16 ppm (Figure 10B). The peak at 16 ppm can

(75) Blümel, J. *J. Am. Chem. Soc.* **1995**, *117*, 2112–2113.

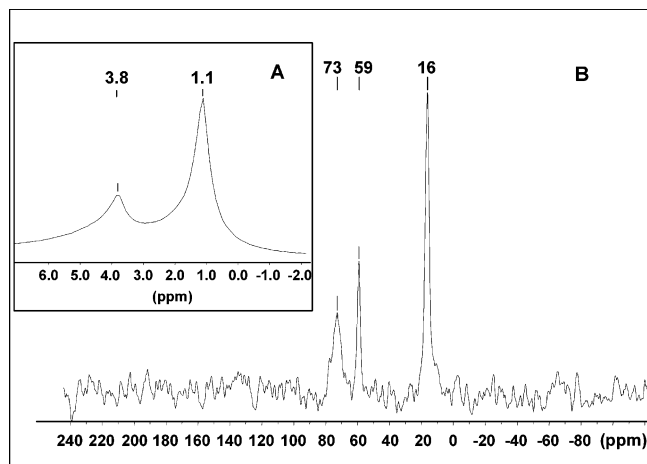


Figure 10. NMR spectra of the solid resulting from the reaction at room temperature of ethanol with $\equiv\text{SiO-TiNp}_3$ synthesized on $\text{SiO}_{2-(500)}$: (A) ^1H MAS NMR; (B) ^{13}C CP-MAS NMR.

be attributed to the methyl carbon, while the two signals at 73 and 59 ppm correspond to the methylene carbon $\text{O-CH}_2\text{-}$ of ethoxy groups. The presence of these two peaks shows that at least two ethoxy species exist on the surface. The signal at 73 ppm is attributed to the methylene carbon of ethoxy ligands σ -coordinated on Ti, $\equiv\text{Ti-OCH}_2\text{-CH}_3$, and the signal at 59 ppm to the methylene carbon of a silicon ethoxide, $\equiv\text{Si-OEt}$, formed by reaction of surface silanol groups with ethanol, as observed by Blümel,⁷⁵ and to the methylene carbon of a few ethanol molecules H-bonded to residual silanols or coordinated on titanium. However strong EtO-H or EtO-D stretching bands are not seen by IR in Figure 9.

All these data are consistent with the formation of a monosiloxytrisethoxy titanium complex, $\equiv\text{SiOTi(OEt)}_3$ ($\mathbf{3a}_{\text{OEt}}$), on the $\text{SiO}_{2-(500)}$ support, in agreement with the results obtained in the case of the reaction with methanol.

Reaction of the $(\equiv\text{Si-O})_n\text{Ti(Np)}_{4-n}$ Species ($n = 1, 2$) with *tert*-Butanol. When the surface alkyl complex $\mathbf{2a}$ supported on $\text{SiO}_{2-(500)}$ was exposed to $^t\text{BuOH}$ vapor (40 Torr) at room temperature, the yellow solid turned white. The reaction was followed by infrared spectroscopy (Figure 11). The $\nu(\text{C-H})$

and $\delta(\text{C-H})$ vibration bands characteristic of neopentyl ligands apparently disappeared after reaction with *tert*-butyl alcohol and were replaced by new $\nu(\text{C-H})$ (2976, 2931, 2905, and 2872 cm^{-1}) and $\delta(\text{C-H})$ (1470, 1458, 1388, and 1364 cm^{-1}) bands, which can be attributed to *tert*-butoxy ligands. The $\nu(\text{O-H})$ vibration band of free silanols was not recovered, and the band corresponding to hydrogen-bound silanols slightly decreased in intensity. This indicates that *tert*-butyl alcohol may react with, or be coordinated to, those hydrogen-bound silanols near or at the silica surface.

Neopentane was the only gas liberated, and the NpH/Ti ratio was found to be 2.6 for a sample prepared on a larger scale. It was only slightly lower than would be expected in the case of a total reaction of $\mathbf{2a}$ with *tert*-butyl alcohol to give a presumed $\equiv\text{SiOTi(O}^t\text{Bu)}_3$ -supported complex on $\text{SiO}_{2-(500)}$. The elemental analysis of the supported complex obtained by reaction between $\mathbf{2a}$ and $^t\text{BuOH}$ gave a ratio $\text{C/Ti} = 13.2$. The result expected in the case of three *tert*-butoxy ligands is 12. The small excess may be attributed to $\equiv\text{Si-O}^t\text{Bu}$ surface species and to a few $^t\text{BuOH}$ molecules (less than 0.3 per Ti) H-bonded to residual silanols or coordinated to the titanium of the presumed alkoxy surface complex, $\equiv\text{SiOTi(O}^t\text{Bu)}_3$, as proposed above for ethanol. However no strong $^t\text{BuO-H}$ stretching bands are observed by IR in Figure 11.

Solid state ^{13}C NMR of this complex showed a single intense peak at 31 ppm and no peak at 36 ppm (corresponding to the quaternary carbon of a surface titanium alkyl $\equiv\text{TiCH}_2\text{CMe}_3$). This peak is reasonably attributable to the methyl groups of the *tert*-butoxy ligands. The quaternary carbons of these ligands were not observed in these conditions.

After reaction of the $(\equiv\text{SiO})_n\text{TiNp}_{4-n}$ species $\mathbf{2a}$ ($n = 1$) and $\mathbf{2b}$ ($n = 2$) supported on $\text{MCM-41}_{(500)}$ with *tert*-butyl alcohol in the same conditions, the analysis of the gas phase evolved during the exchange reaction showed only neopentane in a ratio $\text{NpH/Ti} = 2.4$, which is the value expected in the case of a total ligand exchange of the neopentyl by *tert*-butoxy groups in the case of a $\text{MCM-41}_{(500)}$ support. The titanium and carbon elemental analysis gave a ratio $\text{C/Ti} = 11.8$. The expected result would be 9.6 for a $(\equiv\text{SiO})_{1.6}\text{Ti(O}^t\text{Bu)}_{2.4}$ formulation. The quite high value may be attributed as previously to the presence of $\equiv\text{Si-O}^t\text{Bu}$ surface species and to $^t\text{BuOH}$ molecules (less than

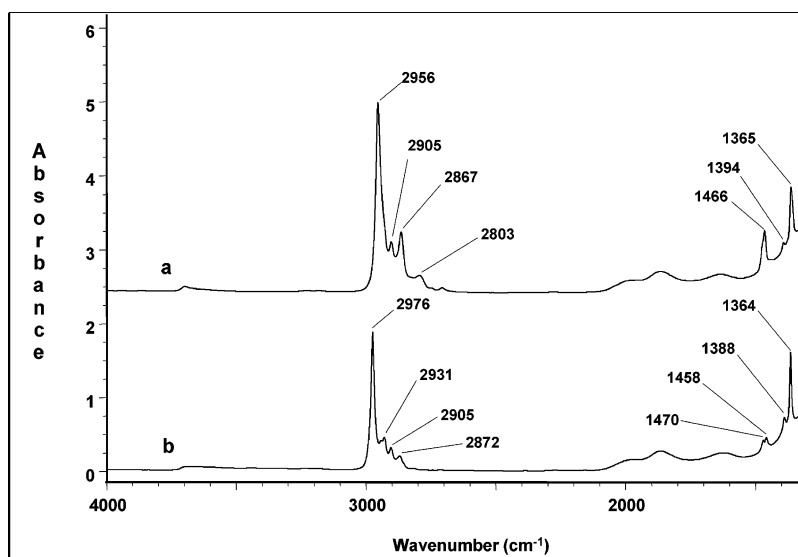


Figure 11. Reaction between $\equiv\text{SiOTiNp}_3$ synthesized on $\text{SiO}_{2-(500)}$ and *tert*-butyl alcohol followed by IR: (a) $\equiv\text{SiOTiNp}_3$; (b) a after exposure to *tert*-butyl alcohol (40 Torr) at room temperature for 3 h and thermal treatment at 70 °C under vacuum (10^{-4} mbar) for 3 h in the presence of a cold trap at 77 K.

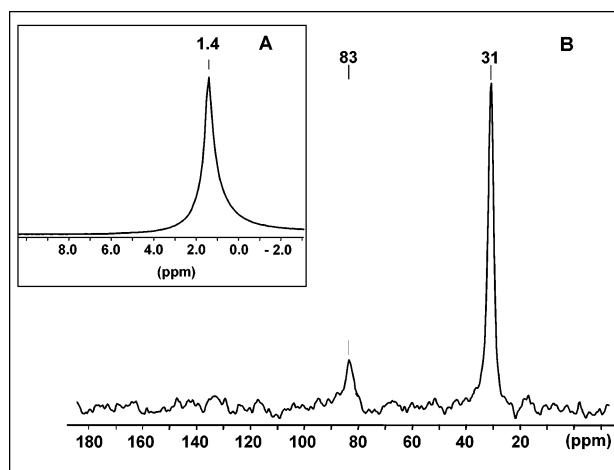


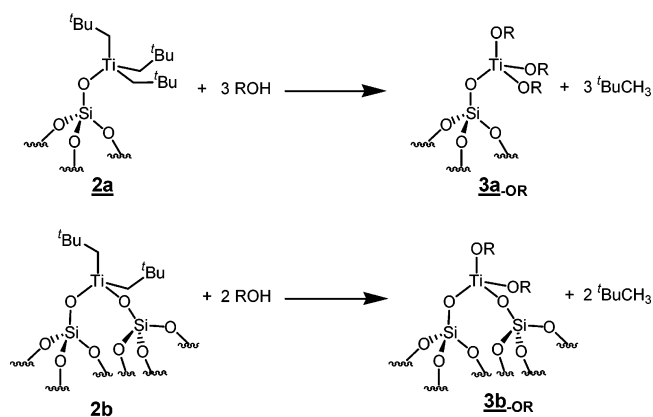
Figure 12. NMR spectra of the solid resulting from the reaction at room temperature of *tert*-butyl alcohol with **2a** and **2b** supported species synthesized on MCM-41₍₅₀₀₎: (A) ¹H MAS NMR; (B) ¹³C CP-MAS NMR.

0.6 per Ti) H-bonded to residual silanols or coordinated to the titanium alkoxide surface complexes. The solid state NMR spectra (Figure 12) were better resolved compared to those of SiO₂-(500), due to the higher complex loading (4 instead of 1.3 wt % Ti). The ¹H spectrum (A in Figure 12) shows a unique broad peak centered at 1.4 ppm, which is assigned to the protons of the methyl groups of *tert*-butoxy ligands. Solid state ¹³C NMR (B in Figure 12) shows a signal at 31 ppm attributed to carbon of the methyl groups and a signal at 83 ppm corresponding to the quaternary carbon, -OC(CH₃)₃, of *tert*-butoxy ligands. This last signal is downfield compared to the free alcohol (ca. 69 ppm), due to the Ti-OC(CH₃)₃ σ -coordination.

The XANES spectrum of the solid resulting from the reaction of *tert*-butyl alcohol with **2a** and **2b**, synthesized on MCM-41₍₅₀₀₎, is shown in part b of Figure 6. A sharp and intense pre-edge peak is also observed, at 4969.8 \pm 0.3 eV with a normalized height of 0.70 (half-height width of 1.5 eV). The spectrum does not differ significantly from spectrum 6a, which indicates that titanium seems also present as four-coordinated Ti(IV) in the material after treatment with *tert*-butyl alcohol.

In Figure 13 are shown the experimental and fitted EXAFS signals obtained for the complexes resulting from the reaction of *tert*-butyl alcohol with **2a** and **2b** supported onto MCM-41₍₅₀₀₎. The data are consistent with an average of 4.0 oxygen atoms at 1.80(1) Å (with a k^1 weighting the results of the fit do not change much: 4.0 O at 1.79(1) Å, $\sigma_{\text{O}}^2 = 0.0048(8)$ Å²). This distance is in good agreement with values obtained from

Scheme 3. Reaction of **2a** and **2b** Silica-Supported Complexes with an Alcohol (R = Me, Et, ^tBu)



crystallographic data for Ti-OSi \equiv (see above) and Ti-O^tBu (1.735 to 1.820 Å for heptadecakis(*tert*-butoxy)hydroxoheptacosaoxaoctadecatitanium *tert*-butyl alcohol solvate⁷⁶). Moreover, two additional shells could be tentatively added to improve the fit, one including carbon at 2.98 Å, corresponding to the nonbonding quaternary carbon atoms of the *tert*-butyl ligands (this distance lies in the 2.96–3.14 Å range obtained for similar Ti \cdots C distances found in titanium tetramethoxide crystal⁷⁷), and the other silicon at 3.46 Å, corresponding to the silicon atoms of \equiv SiO-Ti moieties. The inclusion of these extra parameters decreased the quality factor, $(\Delta\chi)^2/\nu$, from 1.4 ($\nu = 17$) to 1.3 ($\nu = 13$). The EXAFS-derived parameters are collected in the second part of Table 2.

All these observations are consistent with the formation of new silica-supported tetrahedral titanium complexes, characterized as a monosiloxytris-*tert*-butoxy titanium, \equiv SiO-Ti(O^tBu)₃ (**3a_{OR}**), on SiO₂-(500) and a mixture of \equiv SiO-Ti(O^tBu)₃ (**3a_{OR}**) and (\equiv SiO)₂Ti(O^tBu)₂ (**3b_{OR}**) complexes on MCM-41₍₅₀₀₎ (Scheme 3).

6. Reaction of (\equiv SiO)TiNp₃ with Oxygen. The surface complex (\equiv SiO)TiNp₃ (**2a**) is known to be highly sensitive to oxygen, and reactions are generally conducted in the absence of oxygen or air. We wished to systematically study the reactivity of (\equiv SiO)TiNp₃ toward dry molecular oxygen. The alkyl complex supported on SiO₂-(700) was exposed to dry oxygen (400 Torr) at room temperature. The reaction was followed by infrared spectroscopy and the complex obtained finally characterized by solid state MAS NMR, chemical analysis, and analysis of the gas phase. The gas phase was analyzed by volumetry and gas phase chromatography.

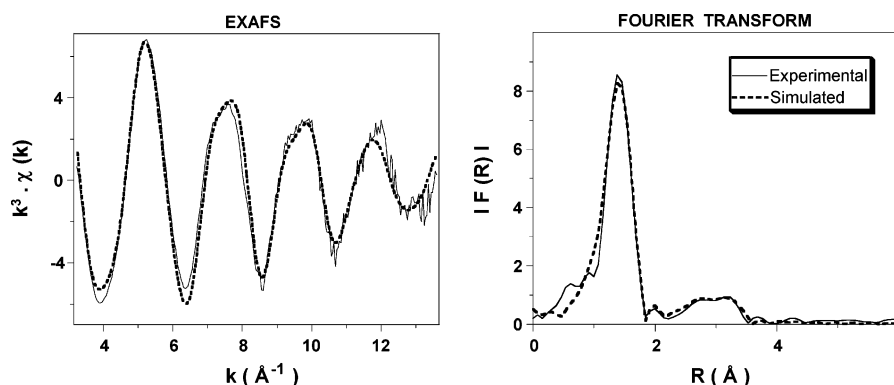


Figure 13. Ti K-edge k^3 -weighted EXAFS (left) and Fourier transform (right) of the solid resulting from the reaction of *tert*-butyl alcohol with the (\equiv SiO)_nTiNp_{4-n} complexes ($n = 1$ or 2) synthesized on the MCM-41₍₅₀₀₎ support and comparison with the simulated curves. Solid lines: experimental. Dashed lines: spherical wave theory.

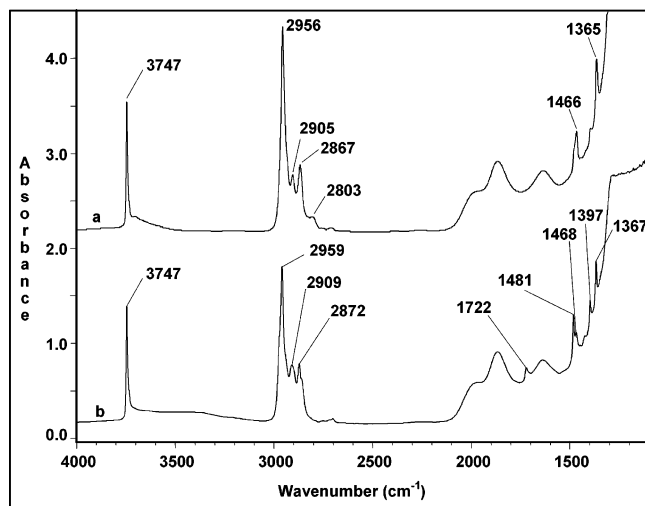


Figure 14. Reaction between $\equiv\text{SiO-TiNp}_3$ synthesized on $\text{SiO}_2-(700)$ and molecular oxygen followed by IR: (a) $\equiv\text{SiO-TiNp}_3$; (b) a after exposure to dry O_2 (400 Torr) at room temperature for 3 days.

A visible color change and infrared spectroscopy indicate that the surface alkyl species reacts slowly with molecular oxygen at room temperature. The yellow solid becomes perfectly white over several hours.

The in situ IR spectrum of the complex obtained after the reaction of **2a** and molecular oxygen at room temperature shows the disappearance of vibration bands corresponding to neopentyl ligands and the formation of bands characteristic of new supported species (Figure 14). The $\nu(\text{C-H})$ vibration bands after reaction are broader than those of the alkyl species: the small band at 2803 cm^{-1} disappeared, and the others shifted slightly (2959, 2909, 2872 cm^{-1} instead of 2956, 2905, 2867 cm^{-1}). The $\delta(\text{C-H})$ vibration bands also shifted from 1466, 1394, and 1365 cm^{-1} to 1468, 1397, and 1367 cm^{-1} , and a fourth band appeared in the region of 1481 cm^{-1} (a new IR band, at 1482 cm^{-1} , also appeared after the reaction of $(\equiv\text{SiO})\text{ZrNp}_3$ with dry dioxygen^{9,50}). A very weak band also appeared at ca. 1722 cm^{-1} , which can be attributed to the $\nu(\text{C=O})$ vibration of an aldehyde. A similar band has never been observed previously with the zirconium-supported complex.

The final product obtained by reaction between $(\equiv\text{SiO})\text{TiNp}_3$ and molecular oxygen has been characterized by ¹H (Figure 15) and ¹³C (Figure 16) CP MAS NMR spectroscopy. The spectra can be compared with the starting material $(\equiv\text{SiO})\text{TiNp}_3$ (Figures 2c and 3c).

The ¹H NMR spectrum, obtained for a sample prepared by impregnation, shows mainly two peaks at ca. 1.1 and 4.2 ppm, which can be attributed respectively to the protons of a methyl group and of a methylene O-CH₂ group. As for infrared spectroscopy, the important shift of the methylene signal, +1.8 ppm, evidences the reaction. A small peak was also detected at 9.8 ppm and might be attributed to the proton of an aldehyde, in agreement with infrared spectroscopy.

The ¹³C CP-MAS NMR spectrum shows three peaks at 88.5, 33.5, and 25 ppm. By analogy with the results obtained from the study of the reaction of $(\equiv\text{SiO})\text{ZrNp}_3$ with dioxygen (three peaks at 82, 32, and 24 ppm)^{9,50} these three peaks can be attributed to the three carbon atoms of a O-Np group (the

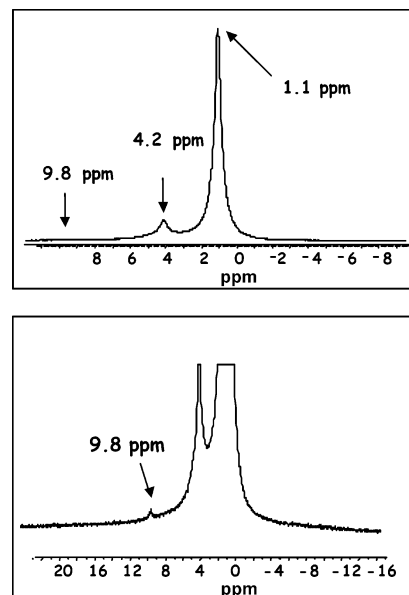


Figure 15. ¹H MAS NMR spectrum of the reaction product of $\equiv\text{SiO-TiNp}_3$ synthesized on $\text{SiO}_2-(700)$ and molecular oxygen.

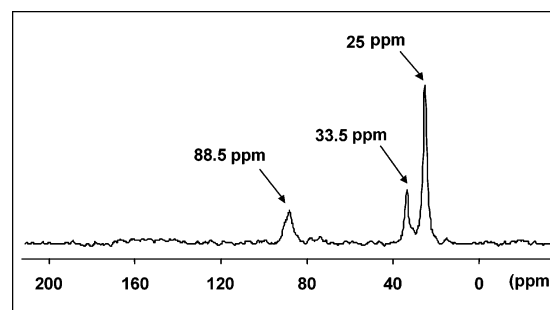


Figure 16. ¹³C CP-MAS NMR spectrum of the reaction product of $\equiv\text{SiO-TiNp}_3$ synthesized on $\text{SiO}_2-(700)$ and molecular oxygen.

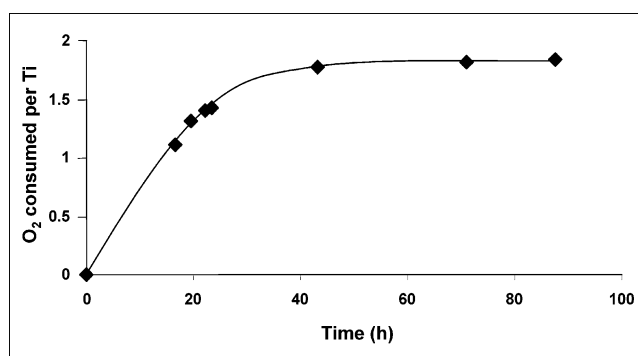


Figure 17. Evolution of the amount of oxygen consumed (O_2/Ti) during the reaction of $\equiv\text{SiO-TiNp}_3$ synthesized on $\text{SiO}_2-(700)$ with molecular oxygen at room temperature.

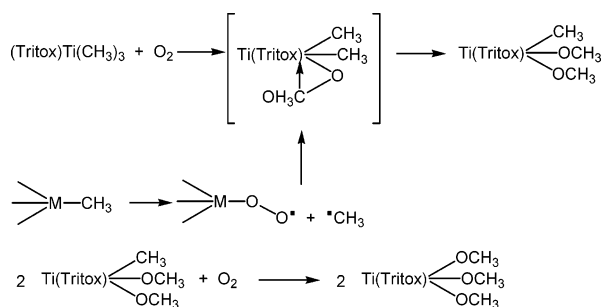
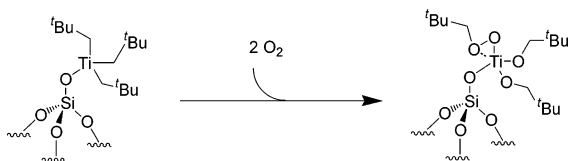
methylene carbon, the quaternary carbon, and the carbon of the methyl group, respectively).

Elemental analysis shows that no carbon has been removed from the sample, the C/Ti ratio being unchanged by reaction with oxygen.

The evolution of the gas phase was followed during the oxidation reaction: Gas phase chromatography failed to detect any gaseous reaction products, so the variation of the gas phase could be related to oxygen adsorption. The consumption of oxygen over time, as determined by volumetry, is shown in Figure 17. The graph is consistent with a slow reaction, which is complete after about 40 h. The global amount of oxygen

(76) Campana, C. F.; Chen, Y.; Day, V. W.; Klemperer, W. G.; Sparks, R. A. *J. Chem. Soc., Dalton Trans.* **1996**, 691–702.

(77) Wright, D. A.; Williams, D. A. *Acta Crystallogr.* **1968**, B24, 1107–1114.

Scheme 4. Proposed Mechanism for the Formation of (tritox)Ti(OCH₃)₃ (tritox = (tBu)₃CO⁻; ref 79)**Scheme 5. Primary Products Possibly Formed during the Reaction of ≡Si-O-TiNp₃ with Oxygen**

adsorbed at the end of the reaction was measured on three different samples and compared with the titanium microanalysis for each sample. The results obtained were successively 1.8, 2.0, and 2.3 mol of O₂ adsorbed per mole of Ti grafted on the surface and are consistent with a stoichiometry of 2 ± 0.3 mol of oxygen adsorbed per mole of monosiloxytrisneopentyl titanium.

All results can be explained by the formation of a trisneopentoxy titanium species on the surface, ≡SiO-Ti[OCH₂C(CH₃)₃]₃, **3a_{ONp}**, as already observed for supported trisneopentyl zirconium species⁵⁰ and consistent with the reported action of dry oxygen on tetra-neopentyl titanium.⁷⁸ The only discrepancies are the amount of sorbed oxygen (2 mol per titanium, while 1.5 mol are expected) and the appearance of small amounts of aldehydes.

The synthesis of trisalkoxy species by reaction of molecular complexes of titanium such as (tBu₃SiO)TiMe₃ with molecular oxygen has been previously studied in the literature.⁷⁹ Several mechanisms were proposed for the formation of the alkoxide species (Scheme 4). η²-Peroxo intermediates may have been obtained either by insertion of oxygen in the M-C bond⁸⁰ or by a radical reaction.⁸¹ The active oxygen of the methylperoxy-metal bond (Ti-O-OMe) is then transferred to the adjacent methyl ligand, via a nucleophilic reaction of M-CH₃ onto the oxygen. In a second step, there is an insertion of a second oxygen molecule in the remaining M-C bond and a bimolecular reaction results in trisalkoxy products.

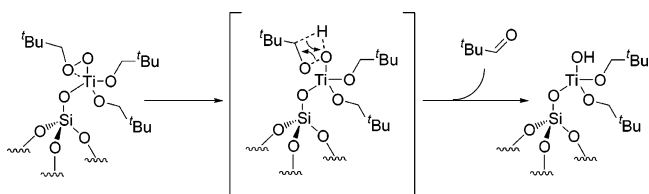
Such a bimolecular mechanism is not possible if the titanium moieties are immobilized by their ≡SiO-Ti link to the surface. It then seems reasonable, by comparison with the data obtained in solution, to suggest that there is formation of ≡SiO-Ti(O-ONp)(ONp)₂, a neopentylperoxobisneopentoxy titanium species (Scheme 5), which cannot evolve rapidly to a trisalkoxide complex. This explains the stoichiometry of the oxygen adsorption, which is in agreement with the formation of this peroxo complex.

(78) Davidson, P. J.; Lappert, M. F.; Pearce, R. *J. Organomet. Chem.* **1973**, *57*, 269–277.

(79) Lubben, T. V.; Wolzanski, P. T. *J. Am. Chem. Soc.* **1987**, *109*, 424–435.

(80) (a) Arlman, E. J.; Cossee, P. *J. Catal.* **1964**, *3*, 99–104. (b) Clawson, L.; Soto, J.; Buchwald, S. L.; Steigerwald, M. L.; Grubbs, R. H. *J. Am. Chem. Soc.* **1985**, *107*, 3377–3378.

(81) Labinger, J. A.; Hart, D. W.; Seibert, W. E.; Schwartz, J. *J. Am. Chem. Soc.* **1975**, *97*, 3851–3852.

Scheme 6. One Possible Mechanism for the Decomposition of the Peroxo Species Obtained after the Reaction of O₂ onto ≡SiO-Ti(CH₂tBu)₃

All attempts to characterize the peroxo function failed, probably because it is not stable. Up to now the experimental data do not give a clear idea of its transformation products. One possibility, which is experimentally supported by infrared spectroscopy and solid state NMR, is the formation of an aldehyde by the mechanism depicted in Scheme 6.

However this reaction scheme is probably not the only one, and radicals are also probably involved in this transformation of the peroxo complex, as in the case of supported trisneopentyl zirconium. The main difference with zirconium is that the peroxo complex is relatively stable in the case of titanium. Additional information obtained by other methods such as ¹⁷O NMR are required to propose more detailed decomposition pathways of the peroxo complex.

Conclusion

This study sought to establish a route to new well-defined silica-supported titanium complexes to be used in oxidation reactions. A silica-supported titanium alkyl has been synthesized by subliming tetrakisneopentyl titanium (**1**) onto an Aerosil silica surface dehydroxylated at 500 °C, SiO₂₋₍₅₀₀₎. Through the use of a large variety of spectroscopic and chemical assays, we are able to propose a single formula, ≡SiO-TiNp₃, **2a**, for this product, consistent with the ≡SiO-ZrNp₃ structure proposed previously for the grafting of ZrNp₄ onto SiO₂₋₍₅₀₀₎.⁹ Quite the same behavior was obtained by using the impregnation method for the grafting of TiNp₄ on SiO₂₋₍₅₀₀₎ and SiO₂₋₍₇₀₀₎. If the silica support is dehydroxylated at a lower temperature (200 °C), a bi-grafted titanium complex, (≡SiO)₂Ti[CH₂C(CH₃)₃]₂ (**2b**), is also formed. On MCM-41 the same conclusions can be drawn, but the formation of multigrafted species also occurs on a support dehydroxylated at 500 °C (MCM-41₍₅₀₀₎); ca. 35% of a monopodal complex, ≡SiO-Ti[CH₂C(CH₃)₃]₃, **2a**, are formed with ca. 65% of a bipodal titanium bisalkyl complex, (≡SiO)₂Ti[CH₂C(CH₃)₃]₂, **2b**, while on MCM-41₍₂₀₀₎, **2b** is almost the only species formed on the surface after the grafting reaction. This behavior is attributed to a different repartition of the silanol OH groups on MCM-41, leading to a shorter distance between them and maybe to steric hindrance effects due to the limited size of the pores of this mesoporous material. The SiO₂₋₍₅₀₀₎-supported monosiloxytrisneopentyl titanium, **2a**, was shown to be thermally unstable: Its ligands are modified when heated above 60 °C, and ≡SiO-Ti bonds are opened when the sample is heated above 200 °C.

The titanium surface complexes reacted quantitatively with water, alcohols, and oxygen. The hydrolysis of (≡SiO)TiNp₃ did not lead to well-defined surface species, but it confirmed the structure proposed for the supported alkyl species. In the case of alcohols a series of alkoxy surface complexes were obtained in which titanium was linked by one (Aerosil SiO₂₋₍₅₀₀₎) or two (major species in the case of MCM-41₍₅₀₀₎) bonds to the silica surface, thus producing ≡SiO-Ti(OR)₃, **3a_{OR}**, and (≡SiO)₂Ti(OR)₂, **3b_{OR}**. The supported titanium alkyl complex,

2a, also reacts with dry molecular oxygen, leading mainly to $\equiv\text{SiO}-\text{Ti}[\text{OCH}_2\text{C}(\text{CH}_3)_3]_3$, **3a**_{ONp}, most probably via a relatively unstable alkyl peroxy surface compound such as $\equiv\text{SiO}-\text{Ti}[\text{OCH}_2\text{C}(\text{CH}_3)_3]_2[\text{OOCH}_2\text{C}(\text{CH}_3)_3]$, resulting from the incorporation of two molecules of oxygen in **2a**.

However, in the context of oxidation catalysts, these species may be particularly susceptible to leaching due to the protolytic cleavage of the unique link or of the two bonds to the silica surface. Thus, it seems interesting to synthesize trissiloxy species, better anchored onto the silica surface. One general method known in the laboratory for the transformation of a monopodal species into a tripodal species is the reaction of the alkyl species with hydrogen to form hydride species: this reaction—for example in the case of silica-supported zirconium alkyl^{9–11,15,17}—proceeds with a reorganization of the silica surface and monosiloxytrisalkyl or bisiloxybisalkyl complexes are transformed into trissiloxyhydride complexes. This reaction will be developed in the second part of this series.

Acknowledgment. We thank Valérie Briois and Stéphanie Belin, for their help during the recording of the XAS data at

beam line D44 at LURE, in Orsay, France. We also thank Alain Michalowicz for the very helpful discussions we had on the analysis of the XAS data. Shell Chemicals and Rhodia are gratefully acknowledged for their financial support and fellowships allocated to F.B. and C.R. (Shell) and R.P.S.A. (Rhodia); the Technische Universität München is also acknowledged for having given the opportunity to E.N. to carry out her Diplomarbeit at LCOMS. This work was also financially supported by CNRS and CPE-Lyon.

Supporting Information Available: Characterization of the MCM-41 support: X-ray powder diffractogram, N₂ adsorption isotherm, and pore size distribution determined by the NDLFT method; IR spectrum of the reaction $\equiv\text{SiO}-\text{TiNp}_3$ (**2a**) with D₂O; IR, XPS, UV–vis, and ¹H MAS NMR spectra of the reaction between $\equiv\text{SiO}-\text{TiNp}_3$ (**2a**) and methanol. This material is available free of charge via the Internet at <http://pubs.acs.org>.

OM050675G